CHALMERS
UNIVERSITY OF TECHNOLOGY

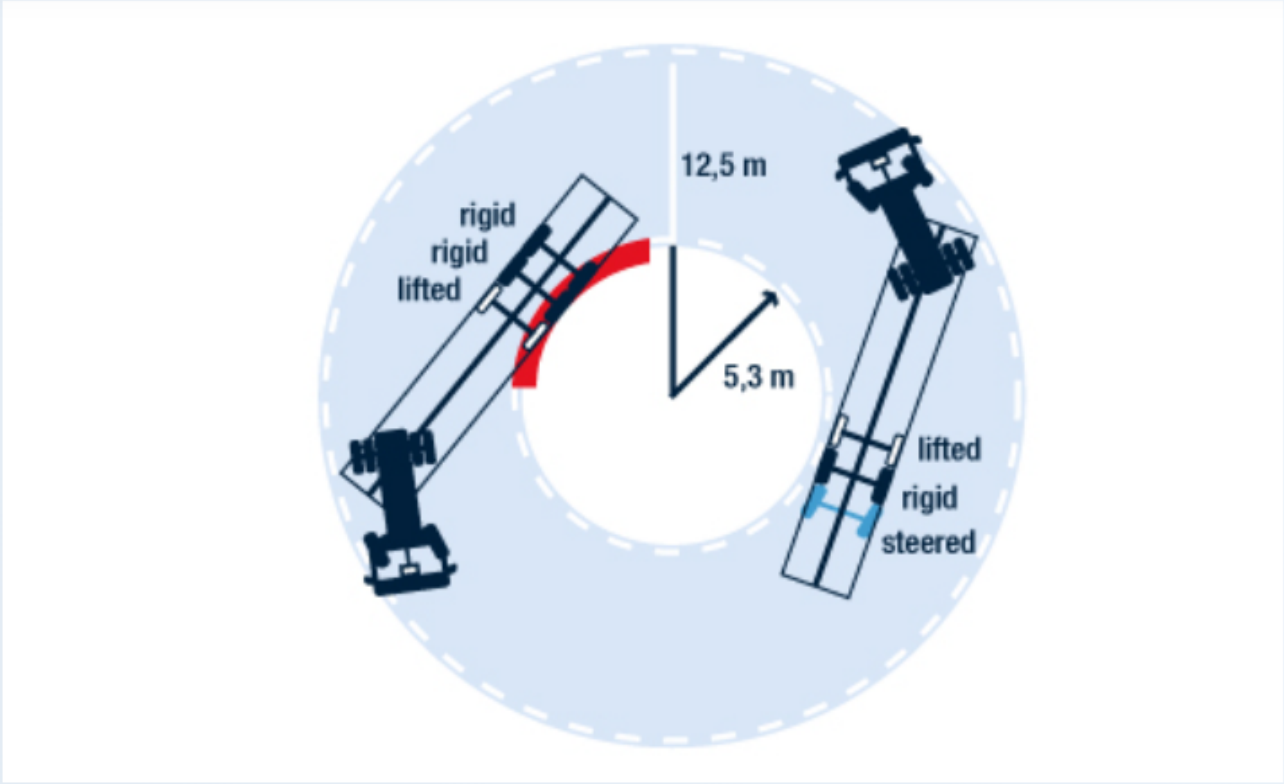

Modelling of steered and lifted axles on long combination vehicles for performance based measures

Master's thesis in Automotive Engineering

Lohith Reddy Keshava Reddy

Department of Mechanics and Maritime Sciences
Chalmers University of Technology
Gothenburg, Sweden 2021

Master's thesis 2021:61

Modelling of Steered and Lifted Axles on Long Combination Vehicles for Performance Based Measures

Lohith Reddy Keshava Reddy

CHALMERS
UNIVERSITY OF TECHNOLOGY

Department of Mechanics and Maritime Sciences
Division of Vehicle Engineering and Autonomous Systems
Chalmers University of Technology
Gothenburg, Sweden 2021

Modelling of Steered and Lifted Axles on Long Combination Vehicles for Performance Based Measures.
Master's thesis in Automotive Engineering

Supervisor: Toheed Ghandriz, *Chalmers University of Technology*; Fröjd Niklas, *Volvo Group Truck Technologies(Volvo GTT)*; Sogol Kharrazi, *Swedish National Road and Transport Research Institute(VTI)*
Examiner: Bengt Jacobson, *Chalmers University of Technology*

Master's Thesis 2021:61
Department of Mechanics and Maritime Sciences
Division of Vehicle Engineering and Autonomous Systems
Chalmers University of Technology
SE-412 96 Gothenburg
Telephone +46 31 772 1000

Cover:BPW steering axles[33]

Typeset in LaTeX
Printed by Chalmers Reproservice
Gothenburg, Sweden 2021

Modelling of Steered and Lifted Axles on Long Combination Vehicles for Performance Based Measures
Master's thesis in Automotive engineering
Lohith Reddy Keshava Reddy
Department of Mechanics and Maritime Sciences
Division of Vehicle Engineering and Autonomous Systems
Chalmers University of Technology

Abstract

High Capacity transport (HCT) vehicles are much more transport efficient compared to conventional heavy goods vehicles. They also contribute to increased energy efficiency and reduction of CO_2 emission. In a recent study by Ghandriz et al., it is shown that long heavy vehicle combinations which are run in heterogeneous fleet results in around 53% reduction in total cost of ownership (TCO) when compared to rigid trucks in homogeneous fleet. [26]
Long combination vehicles (LCVs) can be difficult to operate on city limits because of the tight corners and roundabouts that the vehicle needs to go through. One possible way to evaluate these vehicles is a PBS (Performance Based Standard) based approach in which certain measures with its associated required performance levels are used for assessment of a vehicle combination.

The target for this thesis work is to add low speed steered and lifted axles to the existing models in OpenPBS tool and support the main research project "Performance Based Standards II", by further development of this tool.

Two different methods namely friction-zero side-slip and algorithm-based command steering methods and three different vehicle combinations (Nordic,A-double and Tractor-semitrailer) were considered with semi-trailer axles steered at low speeds. Low speed swept path (LSSP) is considered as the main performance measure of the vehicle to evaluate the effect of steered and lifted axles on semi-trailer at low speeds.
Friction-zero side-slip and algorithm-based command steering methods were implemented and compared. The results show that both methods provide similar percentage improvement of LSSP for all three different vehicle combination. It can be concluded that friction-zero side-slip steering method is a conservative representation of algorithm based command steering method and hence a simple friction-zero side-slip steering method is good enough for representing semi-trailer steered axles in OpenPBS.

For tractor semi-trailer with the last two axles of the semi-trailer steered at low speed, the percentage improvement in the LSSP is 6 % in 90 degree and 8 % in 180 degree turn respectively.
For nordic combination with the last two axles of the semi-trailer steered at low speed, the percentage improvement in the LSSP is 10 % in 90 degree and 15 % for 180 degree turn respectively.

For A-double combination vehicle the percentage improvement in the LSSP with first semi-trailer steered is 13 % and with second semitrailer steered is 7 % in 90 degree turn. The improvement in the LSSP with first semi-trailer steered is 18 % and with second semitrailer steered is 12 % in 180 degree turn.
Temporarily retractable axles were also investigated and it was shown that lifting the second semi-trailer axle improves the percentage of the LSSP by 6 % compared to non-lifted case.

Keywords: *High capacity transport vehicles, Low speed swept path, Performance based standards, Modelica, DYMOLA, OpenPBS tool, Steered axles, Lifted axles.*

Acknowledgements

The Master Thesis work titled "Modelling of Steered and Lifted Axle on Long Combination Vehicles for Performance Based Measures", was carried out during the period February 2021 until July 2021 at Volvo Group Truck Technologies and Chalmers University of Technology.

I would like to express my sincere gratitude to my examiner, professor Bengt Jacobson and academic supervisor Toheed Ghandriz at Chalmers University of Technology. I would also like to thank my industrial supervisor, Niklas Fröjd at Volvo GTT and Sogol Kharrazi at VTI for their continuous support and help during my master's thesis work.

Last but not least, I would like to thank my family and friends who have given me unconditional support during the entire course of Automotive Engineering at Chalmers University of Technology.

Lohith Reddy Keshava Reddy,
Gothenburg, 2021-06-08

Contents

List of Figures

List of Tables

1
Introduction

The introduction to this thesis work is presented in this section consisting of the background, problem statement, methodology and envisioned solution.

1.1 Background

This thesis work is a small part of the main Research project "Performance Based standards II". The major stakeholders of this research project are VTI, the Swedish Road and Transport Research Institute, Volvo GTT, Scania, Nokian, Swedish Transport Agency, Swedish Transport Administration, Chalmers University of Technology and University of Oulu and Parator.

The major and quick rise in the traffic of freight and the congestion they create on highways and city limits are making High Capacity Transport (HCT) solutions more attractive. HCT vehicle bring positive benefits in terms of transport efficiency, energy efficient and CO_2 saving potentials with large economics benefits.

HCT vehicles with payload as high as 74T were introduced in Sweden during April 2018 and allowed length can be expected to increase ffrom 25.25 m in the coming future [21]. One of the ways to regulate heavy vehicles accessibility on road is to use performance based standards [1]. In a PBS scheme limits are set on the performance of the vwhicle rather than setting limits on the length and weight of the vehicle combinations [2].

OpenPBS tool consists of different vehicle models in a modelica language and it includes vehicle parameters for different long vehicle combinations. The vehicle models and vehicle parameters are defined individually to help select any vehicle combination parameters (Nordic, A-double and Tractor-semitrailer) to use them in the vehicle models for simulations. The maneuvers are also defined individually, each maneuver measures a specific performance level of the selected vehicle combination.
The main purpose of this thesis project is to further develop the OpenPBS tool by adding steered and lifted axles for the existing models in Modelica and compare the results by evaluating low speed maneuvers. Also to validate which steering model needs to be implemented by using a performance based measure such as low speed swept path (LSSP) for common different steering concepts.

OpenPBS tool is available on GitHub and it is also an open source which can be used to perform the stability analysis of high capacity transport vehicles in an efficient way. This tool mainly uses Modelica language for modelling and most of the work in this thesis work is done in Dymola [3].

1.2 HCT

High capacity transport vehicles (HCT vehicles) are currently in growing demand. HCT vehicles are more productive and efficient than the regular heavy goods vehicle which are more common. These vehicles consolidate the freight from much smaller trucks, consume lesser fuel and produce lesser emissions per unit cargo transported [26][35]. These combination vehicles are longer and/or heavier than normal truck combinations presently seen. These long combination vehicles will have huge advantage in transportation of containers and goods. Since long combination vehicles has multiple units this can benefit in terms of carrying more load without increasing the gross weight on of individual unit [32]. There will also be decrease in number of vehicles on road which is good for the environment and traffic safety [4].

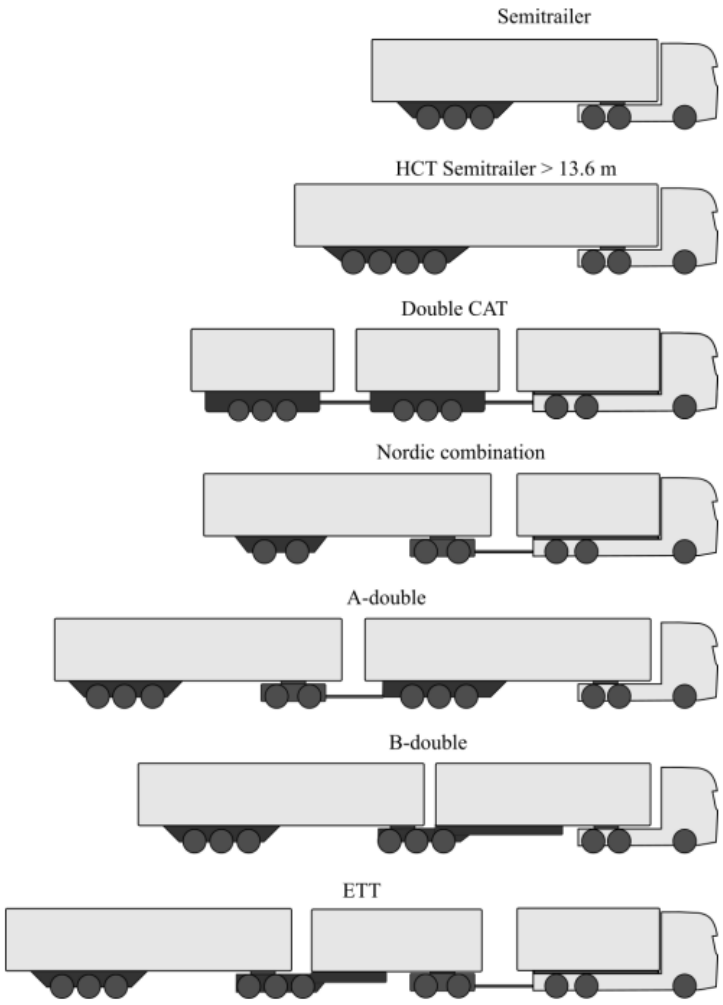

Figure 1.1: Most commonly used HCT combination vehicles, Semitrailer combination as a reference. List from (ISO 18868:2013) updated with combinations used in research projects in Sweden and on the road in Finland [5].

1.3 Performance based standards

Performance based standards (PBS) are set of measures which are designed to evaluate the vehicle stability and on road capabilities and these in turn define the vehicle restrictions. The concept of PBS was first introduced in the 1980's in Canada. The PBS prescribes the vehicle performance characteristics instead of the vehicle design. These characteristics are then used to evaluate the safety of the vehicle and their efficiency. The outcomes or the end targets that should be met are first defined and set by the PBS. Manufacturers can use different approaches to reach these standards. This ensures maximum level of transport efficiency and safety which is the main idea behind PBS [6][16].

1.3.1 Performance based standards around the world

Performance based standards have been implemented in many countries around the world like Australia, New Zealand, Canada etc.
New Zealand is one of the first countries to implement the PBS on heavy vehicles. It dates back to around 1980. In 2002 minimum steady-state rollover threshold (SRT) of 0.35 g was introduced as it was observed that heavy vehicles were involved frequently in rollover accidents. The researchers concluded that low SRT leads to increased frequency in rollover accidents [7] [8]. The primary standards are based on the performance of the worst case standard vehicle which is a 19 m four axle semitrailer [10]. Vehicles meeting that requirement are then assessed using the Australian PBS which are tweaked a little bit.
In Canada, study was performed in 1987 on HCT vehicles with minimum impact on the infrastructure and adequate dynamic performance. The outcome of the research was seven standards to be evaluate the performance [10].

- Static rollover threshold
- Dynamic load transfer ratio
- Friction demand in a tight turn
- Braking efficiency
- Low-speed offtracking
- High-speed offtracking
- Transient high-speed offtracking

The PBS measures described above were used to "create envelope", a set of general vehicle layouts that perform as required. Canada has a perspective approach based on performance standards to HCT vehicle regulations [10].
Australia took a detailed and comprehensive approach in creating PBS for regulation of HCT vehicles. Here the PBS is a voluntary process and is considered as an alternative to perspective regulations [10]. Hence the PBS allows operators to use the vehicles which do not comply with prescriptive limits on mass and dimension, as long as they have performance which comply to the set of standards, having safety, manoeuvrability and infrastructure [10].

1.3.2 Performance based standards in Nordic region

The project “Performance Based Standards II” is currently under work for PBS and its applications in the Nordic Region [11]. The major difference between the PBS in the Nordic region and the other regions is that, the Nordic regions have to consider the snowy and icy road conditions which are generally not significant in other countries [12], which is much more challenging.
PBS was already used in Sweden to regulate the double combination trucks. PBS in Sweden was of keen interest as there was more demand for HCT vehicles since 2013 [10]. Finland uses numerical regression between many simulations. Each simulation uses physically motivated models, but the variation between the used parameters are based on that numerical (non-physical) regression. Turning radius, rear swing and vehicle stability are calculated. Simulations were used to create the equations [15].

1.3.3 Formats of PBS definition

The project “Performance Based Standards II” in Sweden is changing the openness of the PBS measures [11] The projects aims at creating an open source tool available to everyone to use. The concept of OpenPBS is to share physical models of both vehicles and the maneuvers on a standard format , which eliminates the need of numerical regression and more traceable maintenance and development.

1.3.4 Definition of Low speed swept path as performance based standard

Since the thesis study mainly includes the addition of steered and lifted axles the low speed maneuver is the one that is mostly used for all the simulations.

The "LowSpeedcurve " model is defined as a maneuver in OpenPBS which can simulate a vehicle combination to measure three important performance based measures such as low speed swept path (LSSP), tail swing (TS) and frontal swing (FS) of the vehicle combination, defined by the radius of turn and the degree of turn.

The LSSP measure is used most often in this thesis work in the later sections while studying the effect of steered axles and lifted axles and comparing with non-steered and non-lifted axles of the trailing units.

LSSP is defined by [16] as “the maximum width of the swept path between outer most and inner most points of the vehicle combination in a low speed turn with a certain outer radius at a certain friction level and a certain angle between entry and exit”.

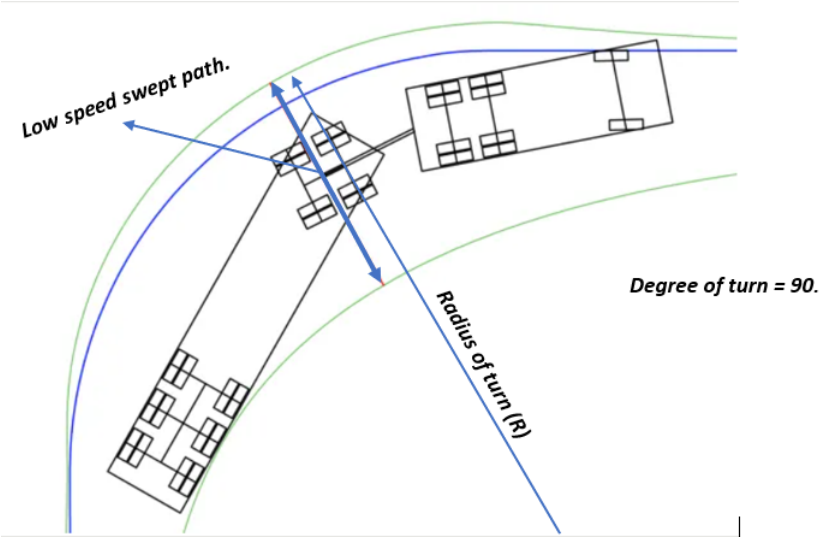

Figure 1.2: Low Speed Swept path [17]

1.4 Modelica and FMI

Modelica is a language that is used to model physical systems. The physical system includes systems like hydraulic, mechanical, electrical etc. Modelica is based on equations and is object oriented. Modelica is a standard language used for physical, acausal and component-based modelling of dynamic systems. There exists modelcia tools which are free of charge as well as those which are commercial. Dymola is a widely used commercial software using Modelica language.

Functional Mock-up Interface, or FMI is an interface or a standard which supports model exchange and co-simulation of dynamic models [32]. A combination of xml-files and compiled C-codes are used in the FMI. The goal of FMI is to improve the exchange of models between OEMs and suppliers.[18]

1.4.1 OpenPBS

OpenPBS tool makes it possible to evaluate and simulate different PBSs for different vehicles. The Swedish transport agency is working on a web based application which is used for approval of individual combination vehicles [31]. OpenPBS may be used in this web based application [1].
The basis of OpenPBS tool is standard formats for dynamic models. The vehicle models used in OpenPBS tool are really simple with low number of parameters yet representing the vehicle behaviour in the relevant accuracy [32]. The manoeuvre models in OpenPBS must also be simple to keep the models understandable and lesser parameters [1].
OpenPBS is built such that all the parameters for simulation in the package can be changed individually [1]. We can conclude that the vehicle model, vehicle definition i,e. parameters, PBS measures and manoeuvres are independent of each other [1]. The advantage of such independent parameters is that all the parameters can be

improved and changed in the future [1].

1.5 Vehicle Dynamics

A single unit vehicle has 6 degrees of freedom (d.o.f) around its centre of gravity. These 6 d.o.f consists of translational and roll movements around the x, y and z axis. The translational d.o.f are often known as vehicle longitudinal, lateral and vertical movements. The rotational d.o.f are known as yaw, roll and pitch movements [19]. A sketch of vehicle axis system is shown in the figure below:

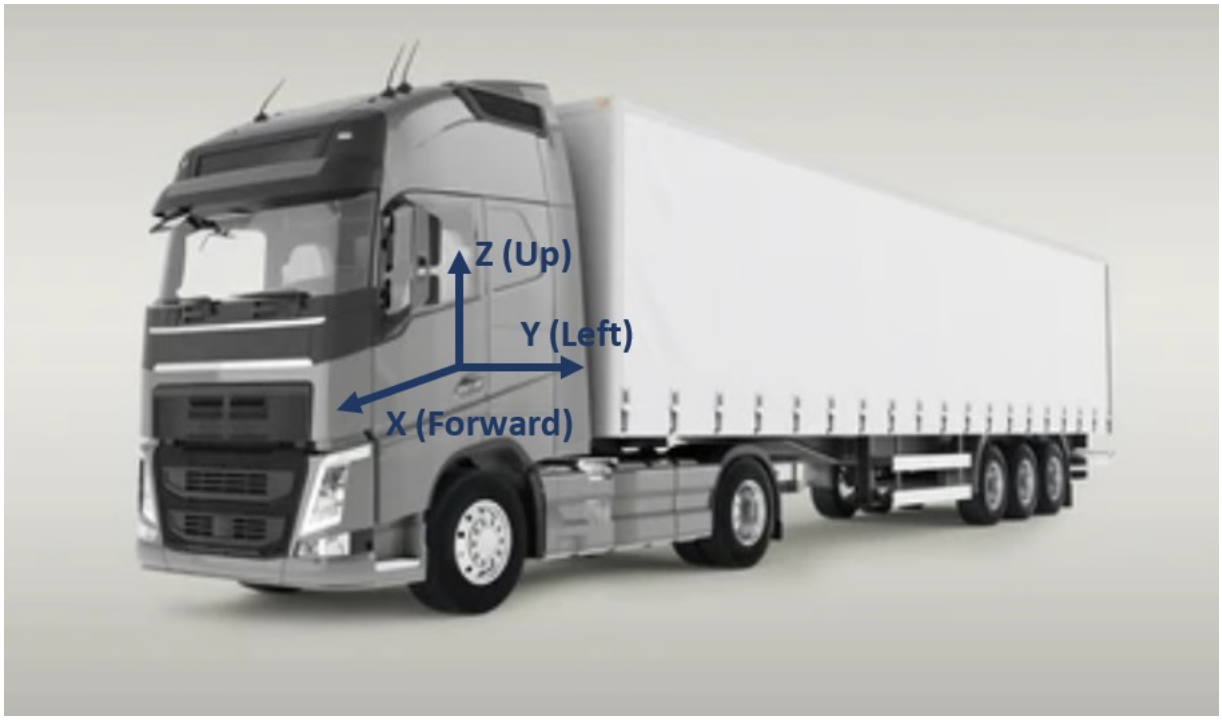

Figure 1.3: ISO 8855 Coordinate system of the truck [24]

Transient state is the time between the steering input given to the steady state motion. This transient state behaviour defines the vehicle handling characteristics. The vehicle should react fast to changes in the steering input and have minimal oscillation while steady state motion is approaching. Vehicles inertia properties must be considered because there is transnational as well as rotational during the transient states. [19]

1.6 Problem Statement Motivating The Project

Long vehicle combinations are always tricky and difficult to operate on city limits because of the tight corners and roundabouts. There are challenges while operating on highways also due to instability at high speeds. Adding low speed steered axle models is important because they will help meet the performance based requirements and easier dynamic handling e.g, reduce low speed off-tracking of long combination vehicles [36]. Adding lifted axles model will result in reducing fuel consumption [37] and improve vehicle performance e.g. startability, gradeability and acceleration capability at both at high speeds and low speeds. This thesis work will add modelling of steered and lifted axles for low speed maneuvers defined, and comparing the performance based measures will be a key take away in terms of Modelling in Modelica.

1.7 Envisioned Solution

As mentioned in the problem statement the envisioned solution will be to add mathematical models for the steered and lifted axles for different long combination vehicles in existing OpenPBS tool and compare the simulation results to propose feasible steering model for OpenPBS tool.

The primary goal is to select as many different steering models as possible. The selected and feasible few steering models will be investigated by running the simulation for different vehicle combinations such as Tractor-Semitrailer, Nordic and A-double and the results will be compared based on the performance measure i,e LSSP. The final goal in modelling steered axles is to propose the feasible steering method that will best fit in the OpenPBS tool compared to different steering methods that are simulated.

To investigate the effect of steering models at low speed, the Low-speed curve maneuver is considered which measures the LSSP of the vehicle around the defined curve/maneuver and the simulation results of the semi-trailer steered models are compared with each other and they are also comapred with non-steered case.

1.8 Deliverables

Deliverables for this thesis project are listed below.

- To propose how lifted axles should be included in the existing models and integrate the lifted axles to the existing OpenPBS tool in modelica.
- To propose how low speed steered axles should be included in the existing models and integrate the steered axles to the existing OpenPBS tool in modelica..
- To release the updated version of OpenPBS tool to the Gitlab.
- To update front-end calculator (python) to include additions for low speed steered and lifted axles.

2

Literature Study

2.1 Literature study for different steering strategies for semi-trailer

There are many research papers that address the issue of maneuverability and increase in low speed swept path for long vehicle combinations at low speeds. Some of the different steering methods/strategies are discussed in the following section to better understand and choose the feasible solution discussed in those papers.

In Odhams et al research paper [25], a tractor semi-trailer with active steering that controls the steering angle on the semi-trailer is selected. The active steering system works based on the control strategy which is defined as path following. The reference yaw rate and the side slip angle of the fifth wheel is recorded and the same is used as feedback to the controller to calculate the required steering angle to achieve the reference values and semi-trailer axles are steered by the controller so that the rear of the vehicle follows fifth wheel coupling.
This study involves both factors such as different path and different speeds defined. This steering control strategy will improve the low speed maneuverability, off tracking and tyre wear of vehicle combination and also it increases the high speed stability with performance measures such as rearward amplification and reduce the roll over at high speeds [25].

We can notice there are few similarities in what this thesis and the research study [25] is trying to achieve which includes addition of semi-trailer steering system and to improve low speed maneuverability, but this thesis most importantly aims at having a simple steering model which is not the case with the research study in [25]. In [25] more complex active steering with path following steering controller is used which will be a complex model to implement in OpenPBS tool which is Modelica based and this requires a reference model for the path following controller. This will be a bit of complex method to be used in the OpenPBS at present. But the main take away from this study will be that the semi-trailer axles are steered based on the path of the fifth wheel coupling.

There are few studies that try to solve only low speed problem and there are few studies which solve only high speed problem of long combination vehicles. Kural et al in research study [28] mainly concentrates on solving both low speed maneuverability and high speed stability problem of long combination vehicles by proposing

a systematic approach.
The highlight of this semitrailer control strategy is that same control structure is used for different speeds in the range [1-90] km/h using a gain scheduled feedback and feedforward controller [28]. A rigid truck, dolly and semitrailer vehicle combination is selected based on a recent research [29] because it is considered as potential candidate for most efficient means of raod transport after 2020. This study formulates the control problem which aims in minimizing the swept path and also ensuring zero tail swing at low speeds and aims to reduce the rearward amplification at high speeds.
The objectives of the control problem is achieved by initially formulating it as path following and then transforming it into tracking problem using the reference model [28]. This study also explains about the control theory related solution for semitrailer steering at both low speed and high speeds, but in OpenPBS the aim to add steered axles models only at low speeds.

The research study in [27] mainly includes an active steering which is controller based. The LQR controller is designed to improve the maneuverability at low speeds and lateral stability at high speeds of the whole vehicle combination [27]. This study was based on a tractor-semitrailer with three degree of Freedom (3 DOF) linear model. This study uses simulated annealing particle swarm optimization (SAPSO) algorithm to identify key model parameters that are required such as desired yaw rate for the controller. The active steering controller is designed in such a way that it will follow the desired yaw rate and it also aims at reducing the side-slip angle of the units at centre of gravity (CoG). The study in [27] also concludes to have better results in vehicle maneuverability at low speeds and lateral stability at high speeds with active steering controller.

There are many passive steering systems for articulated vehicles developed few of them are defined by [20] as self steering system, command steering system and pivotal bogie systems. These semi-trailer systems will be studied in detail in the following methodology section. These type of semi-trailer steering system steer the axles based on pure geometric relationship which is simple and feasible to model in OpenPBS which is modelica.

2.2 Theory

The passive semi-trailer steering systems can be grouped into three types namely self steering system, command steering system and pivotal bogie systems [20]. Every system will steer the semi-trailer axles with different strategy to find the steering angle that is required to make the turn defined by the front axle. The self-steering system will steer in relation to the lateral tyre forces, the command steering system steers in relation to the articulation angle and the pivotal bogie system steers in relation to the angle of the rear bogie [20]. Every steering system mentioned by [20] works on different principle but every system aims at steering the semi-trailer axles. The principle behind self-steering and command steering systems are studied in detail in the following section and one of them is selected to study in this thesis

work.

2.2.1 Self Steering system

This type of steering system is similar to the conventional steering axle but with a positive trail [20]. The steering control is neither from the driver nor from any actuator when a vehicle is in a low speed turn, the axles are self steered by aligning the axles to the travel direction. This reduces the lateral forces acting on the self-steered axle doneand also in the axle group. This system also help in reducing tyre wear and the also improves low speed maneuverability of the vehicle. Steering angle for the self steered axles is calculated based on the moment balance around the king pins during a maneuver. LeBlanc et al [30] showed that self steering axles generally have a nonlinear relationship between the steer angle and the lateral tyre force as shown in figure 2.1 The equations that govern the non -inear relationship is represented as follows.

$$\delta = \begin{cases} \frac{F_y}{K_1}, & |F_y| < F_{yc}, \\ \frac{F_y}{K_2} + \frac{F_{yc}}{K_2}(1 - \frac{K_2}{K_1}), & |F_y| > F_{yc}, \end{cases} \text{[20]}$$

Where,
F_y = Total lateral force on the axle[N].
F_{yc} = Centering force[N].
δ = Steering angle[rad].
K_1&K_2 = Axle Cornering Stiffness [N/rad].

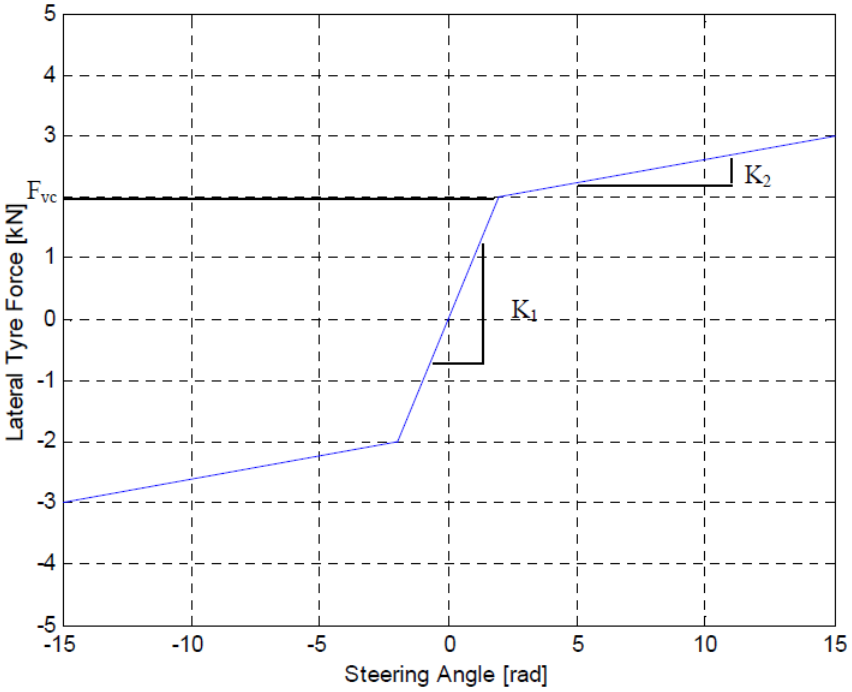

Figure 2.1: Self Steering Axle Lateral Tyre Force vs Steer Angle Relationship [30]

2.2.2 Command Steering system

In a typical command system the rear fixed axles in the tri-axle semi-trailer group are replaced with the conventional style steering axles [20]. The steering angle is determined in relation to the articulation angle between the leading unit and trailing unit of the vehicle combination selected. The equations that govern the command steer system, according to [20] when a vehicle is in a low speed turn, as shown in the figure 2.2 are as follows.

$$\delta_m = arctan\left(\frac{d * sin(\tau)}{b * cos(\tau) - a}\right) \tag{2.1}$$

$$\delta_r = arctan\left(\frac{2 * d * sin(\tau)}{b * cos(\tau) - a}\right) \tag{2.2}$$

where,
δ_m = Semi-trailer middle axle steering Angle [rad].
δ_r = Semi-trailer rear axle steering Angle [rad].
τ = Articulation angle [rad].
d = Distance between trailer axles [m].
b = 5^{th} wheel pin to front trailer axle distance [m].
a = 5^{th} wheel to rear tractor axle distance [m].

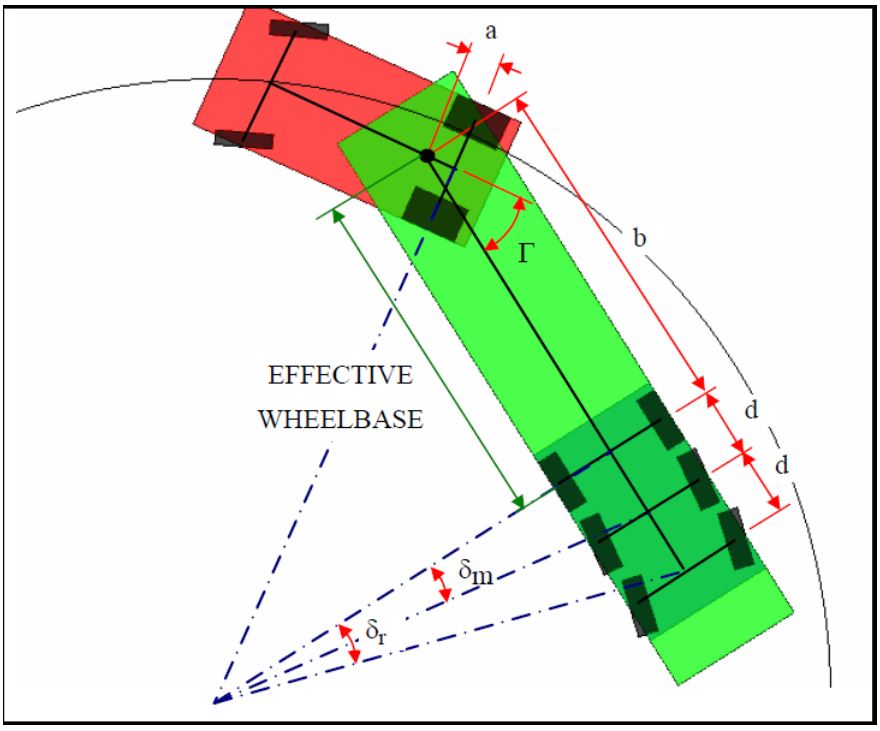

Figure 2.2: Command Steer Low Speed Geometry [20]

Since both rear axles that are selected to steer generate no lateral forces in a turn they can be neglected and the wheelbase of the semi-trailer is reduced to that of an equivalent fixed single axle semi-trailer [20], as indicated in figure 2.2.

In a tractor semi-trailer vehicle combination considered in [20], as seen in the figure 2.2, the tractor has only two axles and parameter 'a' in the governing equation 2.1 & 2.2 can be directly calculated. The parameter 'a' is the geometric distance between the rear axle of the tractor to the fifth wheel coupling.
The tractor considered in OpenPBS tool has three axles with tandem axle on the rear. Hence there is a need to find the parameter 'a' which cannot be obtained directly from the geometric measurements of the tractor. To find the parameter 'a', we first find the point where there is no side slip from the COG as reference and define it as zero side slip point. The distance from this zero side slip point to the fifth wheel coupling is the parameter 'a' used in the current study.

3
Methodology

This thesis work focuses on addition of two important aspects to the existing OpenPBS tool in terms of modelling of steered and lifted axles.

3.1 Semi-trailer Steered Axles

As we know the first axle of any vehicle is steered based on the driver input to axle, but in this thesis work apart from the steering input from driver the semi-trailer steering inputs/steering commands are studied which are based on the kinematic relations of the vehicle combinations. The detail study of the different steering methods are explained in the following section.

3.1.1 Different Steering Models

The two different type of steering model that will be investigate in this thesis are discussed below in detail and the feasible one will be selected based on the results to be implemented in OpenPBS tool in the following sections.

3.1.1.1 Friction Steer/Zero Side-slip Steering Model

As name suggest this steering method will follow the principle of having zero side-slip on the axles of the semi-trailer that are defined to be steered.
The steering model is added using the lateral slip equation 3.1 as defined by [23]. The lateral slip equation 3.1 is the relationship between the slip angle(α), side slip(β) and delta(δ) as shown below.

$$\alpha_{i,j} = \frac{V_{y_{(i,j)}} + (\omega_{z(i,j)} * L_{CoG(i,j)})}{V_{x(i,j)}} - \delta_{i,j} \tag{3.1}$$

When,

$$\alpha_{i,j} = 0 \rightarrow F_{y(i,j)} = 0 \rightarrow \delta_{i,j} = \beta_{i,j} \tag{3.2}$$

The equation for steering angle on the semi trailer axles that are defined as steered is obtained by then substituting equation 3.2 in equation 3.1. The equation that calculates the required steering angle for the semi-trailer axles for friction steered model is expressed as below.

$$\delta_{i,j} = \frac{V_{y_{(i,j)}} + (\omega_{z(i,j)} * L_{CoG(i,j)})}{V_{x(i,j)}} \tag{3.3}$$

Where,
i = number of unit
j = number of the axle on unit i
$\delta_{i,j}$ = Steering angle of the axle j of unit i [rad].
$V_{y(i,j)}$ = Lateral velocity at CoG [m/s].
$\omega_{z(i,j)}$ = Yaw rate at CoG [rad/s].
$L_{CoG(i,j)}$ = Axle position from CoG [m].
$V_{x(i,j)}$ = Longitudinal velocity at CoG [m/s].

Since modelica follows acausal modelling when the slip angle ($\alpha_{i,j}$) is set zero it will automatically calculates the steering angle for semi-trailer axles that are defined to be steered. This will also make lateral force in the axle to zero and reduce the forces in the axle group. A tractor semi-trailer with one of the trailer axle steered at low speed with friction-zero side-slip is shown in the below figure 3.1.

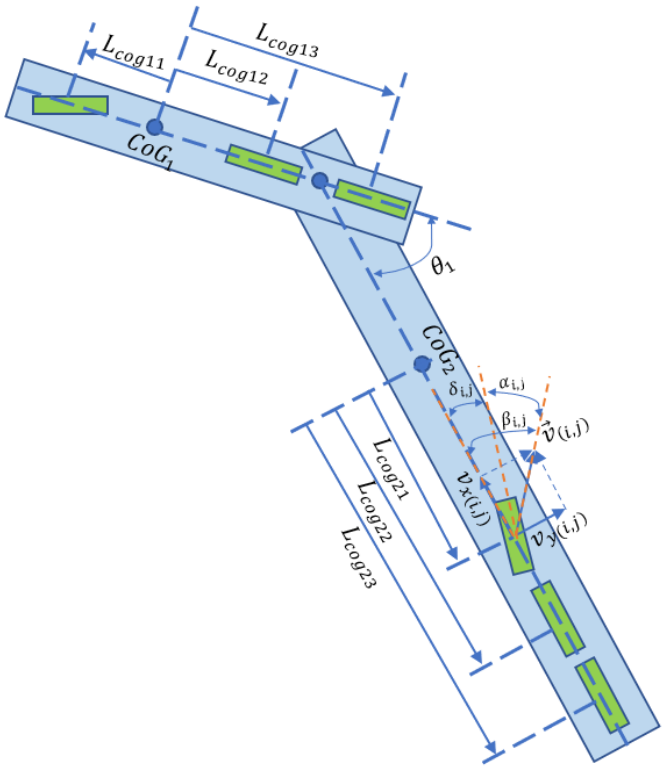

Figure 3.1: Tractor-semitrailer with one axle friction-zero side slip steered

3.1.1.2 Algorithm Based Command Steering

Algorithm based command steering works based on the articulation angle between the leading unit and the trailing unit on which the steering model is added. The articulation angle is sensed using the angle sensor on the fifth wheel or coupling of the vehicle combination and then axles of the semi-trailer are steered in relation to the articulation angle. The underlying assumption is that the low-speed steered axles should be steered so that there is no lateral forces on them if steady state articulation angle and both the leading unit and the trailing unit has same instantaneous center of rotation. This can also be expressed as that the steering angle on the semi-trailer is calculated based on the angle swept by the fifth wheel coupling depending on different vehicle combinations. The relationship between the required steering angle and the articulation angle is non-linear and also includes few of the vehicle parameters as seen in the figure 3.2.

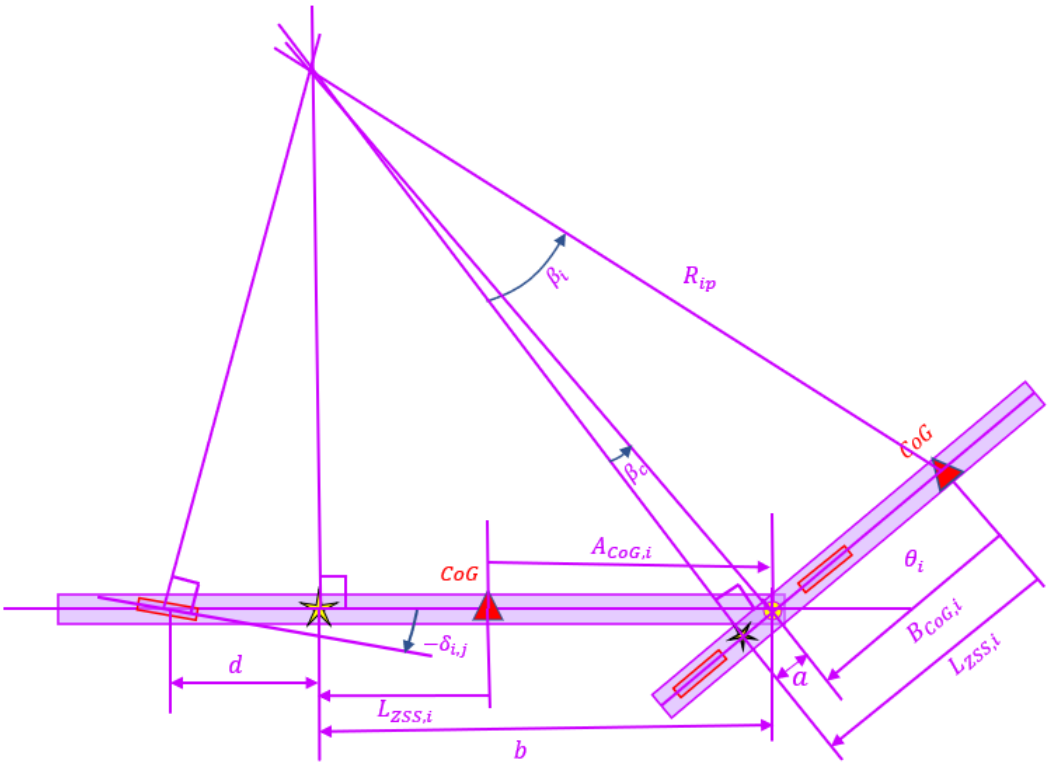

Figure 3.2: Schematic of Tractor-semitrailer with an instantaneous center of rotation used for calculating command Steering

Since the first unit does not have any lead unit, $\delta_{i,j}$ is calculated as if steady state turning with the measured steering angle on the first (manually steered) axle. In this study the low speed steered axles model on the first unit is not studied with algorithm based command steering method.

The general equation governing the algorithm based command steering is as follows.

$$\delta_{i,j} = -arctan\left(\frac{d_{i,j} \cdot sin(\theta_i)}{b_{i,j} \cdot cos(\theta_i) - a_i}\right) \tag{3.4}$$

Where,
i = number of unit
j = number of the axle on unit i
$\delta_{i,j}$ = Steering angle of the axle j of unit i [rad].
θ_i = Articulation angle [rad].
$d_{i,j}$ = Distance between the trailer axles [m].
$b_{i,j}$ = 5^{th} wheel pin to zero side-slip point on trailing unit[m].
a_i = 5^{th} wheel to to zero side-slip point on leading unit[m].

Since both the semi-trailer axles are selected to steer the zero side-slip point is considered on the first semi-trailer axle to have the same instantaneous centre of rotation.
As explained in the theory section the parameter 'a' in the equation 3.4 is calculated in two steps as explained below.
Firstly, the distance from COG to the zero side-slip point is defined as 'a' measure and the distance is calculated using the below equation 3.6 for any vehicle unit.

$$L_{zss_i} = R_{ip} \cdot sin(\beta_i) \tag{3.5}$$

$$L_{zss_i} = \frac{\sqrt{V_{x(i)}^2 + V_{y(i)}^2}}{\omega_{z(i)}} \cdot sin\left(tan^{-1}\left(\frac{V_{y(i)}}{V_{x(i)}}\right)\right) \tag{3.6}$$

Where, i = Number of unit

From figure 3.2 it is seen that parameter 'a_i' is the distance between the fifth wheel coupling point and the zero side-slip point on the leading unit and this can be further calculated with the relationship mentioned in the below equation 3.7 for any vehicle unit.

$$a_i = L_{zss_i} - B_{CoG_i} \tag{3.7}$$

3.1.2 Work Flow

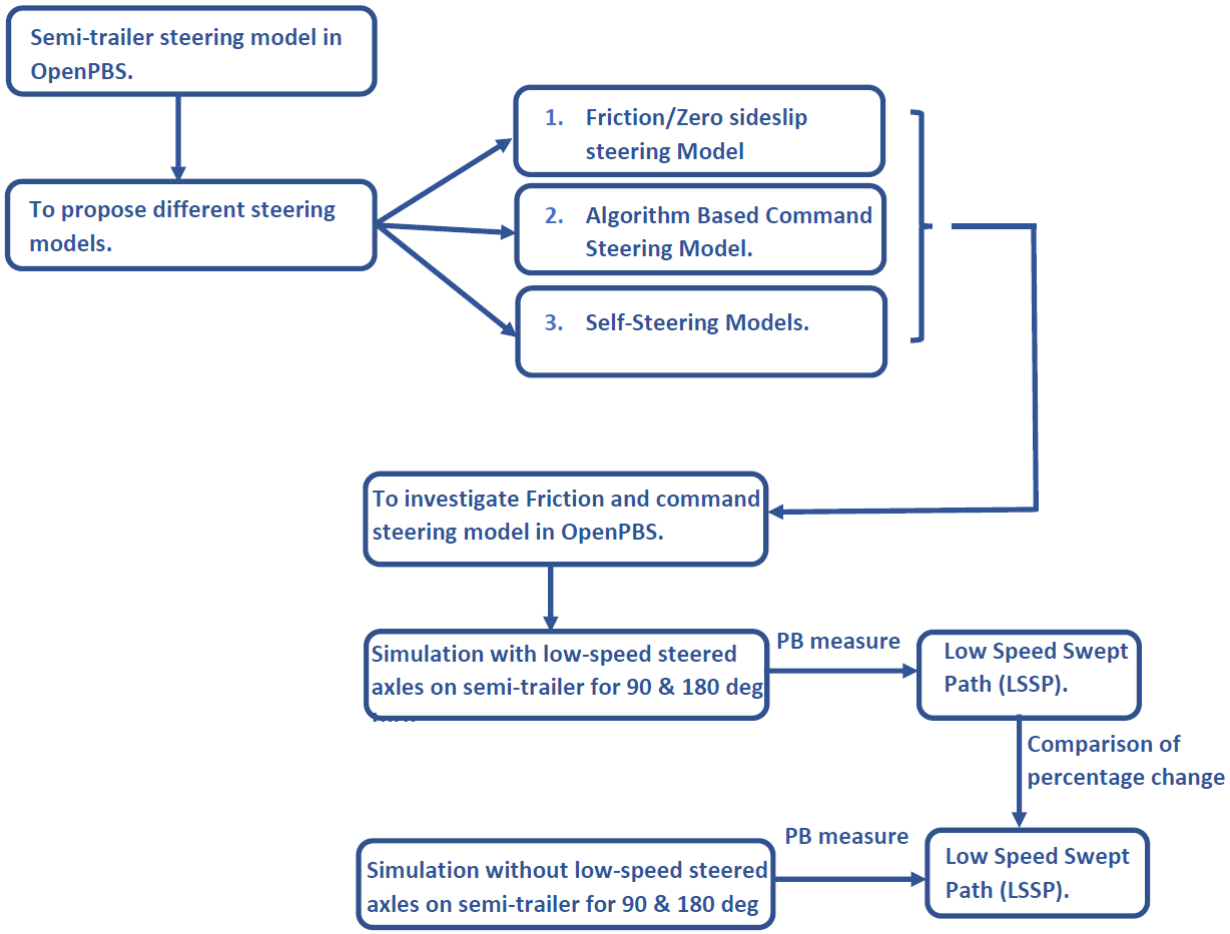

Figure 3.3: Work Flow

The detailed study of steerable axles on semi-trailers of long vehicle combination with effect on low speed swept path is done using OpenPBS tool with work flow as shown in the figure 3.3. The main agenda of the work flow is to investigate the effect of two different semi-trailer steering models and compare the performance based measure (LSSP) of these two models with Non-Steered models in OpenPBS tool using DYMOLA.

The steering model can be added in many different ways as discussed in the literatute study in the previous section. Since the target was to implement the steering model in the OpenPBS tool, it was decided to not have a complex model which uses a reference model or any optimizations techniques to calculate the steering angle of the semi-trailer. To keep it simple and reasonable the friction-zero side-slip steering model and algorithm based command steering model are selected to investigate in detail and the results are shown in the following section. Finally comparing the friction-zero side-slip steering model and algorithm based command steering model, one of these two models will be implemented in the OpenPBS tool based on the feasibility and non-complexity.

Low Speed Swept Path ($LSSP$) is defined by [16] as "the maximum width of the swept path between outer most and inner most points of the vehicle combination in a low speed turn with a certain outer radius at a certain friction level and a certain angle between entry and exit".

For different case study LowSpeedCurve maneuver is selected in the OpenPBS existing tool. The LowSpeedCurve maneuver is defined for 90 and 180 degree curve with keeping radius 12.5 m as constant.

3.2 Lifted Axles

Second target in this thesis work is to model static lifted axles in the existing OpenPBS tool..

Since the vertical forces of different combination vehicles is already recorded, the same vertical forces are used as input parameters to calculate the loaded mass and CoG position of each unit. Modelling lifted axle in OpenPBS is straight forward since the vertical forces is used as input to the models, the vertical force on the axle that is selected to be lifted can be directly set to zero and the vertical forces measured on the other axles can be used as an input to the model if the axles are permanently lifted in a transport mission. If the axles of the semi-trailer are selected to have temporary lifted axles then the new vertical forces on the axles should be calculated and used as input to the model.

3.2.1 Tractor Semi-trailer with Permanently Lifted Axles

Permanently lifted axles on the semi-trailer are quite common and the same is modelled in OpenPBS. The effect of lifted axles on the semi-trailer is studied with Low speed curve maneuvers in the OpenPBS tool.

3.2.2 To Calculate The variation in Vertical Forces (Fz) With Temporarily Lifted Axles

A simple tractor semi-trailer is studied with temporarily lifted axles see section 5.2. The new vertical forces on the non-lifted axles are calculated in MATLAB and used as input parameter in OpenPBS. The below figure 3.4 represents the tractor semi-trailer vehicle combination with no axles lifted.

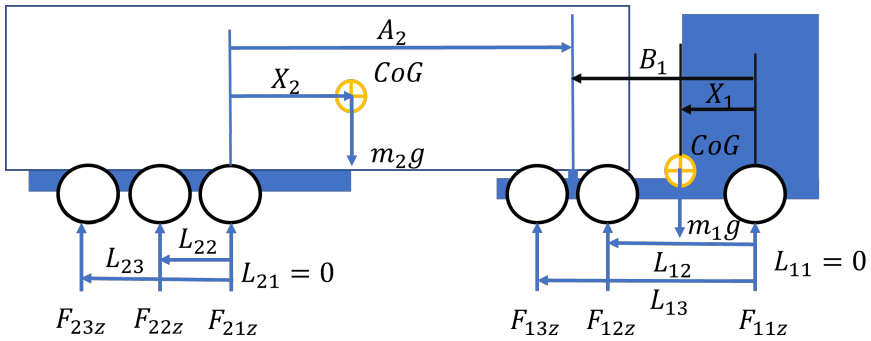

Figure 3.4: Tractor Semi-trailer - With No Lifted Axles

To calculate the new vertical forces on the axles when any axle on the semi-trailer is lifted the most important assumption is the vertical force on $axle_{12}$ & $axle_{13}$ of tractor are equal and the vertical force on $axle_{21}$, $axle_{22}$ & $axle_{23}$ of semi-trailer are equal [34].

$$F_{12z} = F_{13z} \tag{3.8}$$

$$F_{21z} = F_{22z} = F_{23z} \tag{3.9}$$

If any axle on the semi-trailer is lifted the vertical load will be shared by the other non lifted axles. But the amount of load that each axle takes is re-calculated by keeping the CoG position same in both the non lifted and lifted cases. Figure 3.5 shows one of the axles of the semi-trailer is lifted.

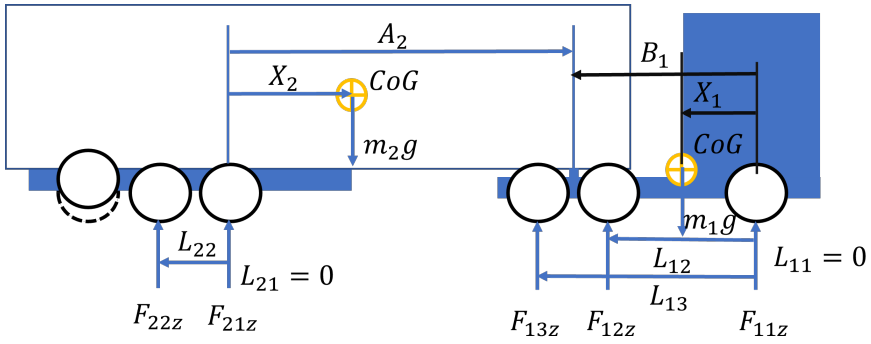

Figure 3.5: Tractor semi-trailer with lifted axles

By considering the assumption made in 3.8 & 3.9 and assuming that the COG position remains the same when an axle is lifted the new vertical forces on each axle is calculated for non-lifted axle on semi-trailer.

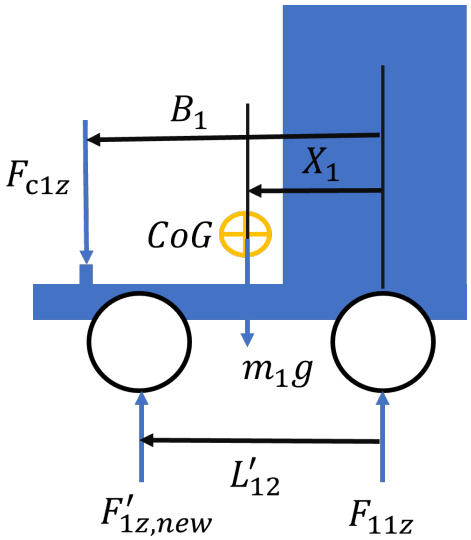

Figure 3.6: Free Body Diagram - Tractor

The mass and moment equilibrium equation of the tractor is as follows

$$\sum F_y = 0 \rightarrow F_{11z} + F'_{1z,new} - F_{c1z} = m_1 g \tag{3.10}$$

$$\sum M = 0 \rightarrow F'_{1z,new} * L'_{12} - F_{c1z} * B_1 = m_1 g X_1 \tag{3.11}$$

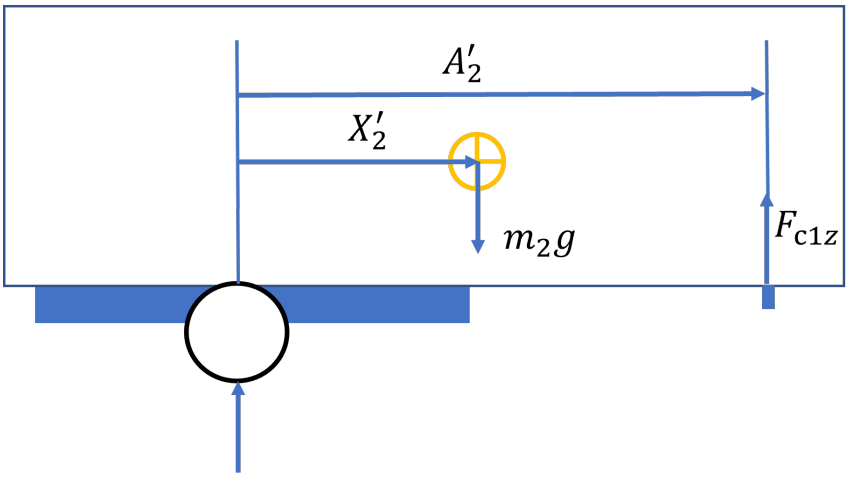

Figure 3.7: Free Body Diagram - Trailer

The mass and moment equilibrium equation of the trailer is as follows

$$\sum F_y = 0 \rightarrow F'_{2z,new} + F_{c1z} = m_2 g \tag{3.12}$$

$$\sum M = 0 \rightarrow F_{c1z} * A'_2 = m_1 g X'_2 \tag{3.13}$$

From the mass and moment equilibrium equations of tractor and semi-trailer the vertical forces and the coupling force can be found solving the algebraic system of equation in matrix form as below [34].

$$AF = B \tag{3.14}$$

The unknowns are F = $[F_{11z},\ F'_{1z,new},\ F_{c1z},\ F'_{2z,new}]$. The matrix A and B can be derived using equilibrium equation 3.10, 3.12, 3.11 & 3.13 as follows.

$$A = \begin{bmatrix} 1 & 1 & -1 & 0 \\ 0 & L'_{12} & B_1 & 0 \\ 0 & 0 & -1 & 1 \\ 0 & 0 & A'_2 & 0 \end{bmatrix} \tag{3.15}$$

$$B = \begin{bmatrix} m_1 g \\ m_1 g X_1 \\ m_2 g \\ m_2 g X'_2 \end{bmatrix} \tag{3.16}$$

Where,

$$F_{12z} = F_{13z} = \frac{F'_{1z,new}}{2} \tag{3.17}$$

$$L'_{12} = L_{12} + \left(\frac{L_{12} + L_{13}}{2}\right) \tag{3.18}$$

If last axle on the semi-trailer i.e, $axle_{23}$ is lifted then

$$A'_2 = A_2 + \left(\frac{L_{22}}{2}\right) \tag{3.19}$$

$$X'_2 = X_2 + \left(\frac{L_{22}}{2}\right) \tag{3.20}$$

$$F_{21z} = F_{22z} = \frac{F'_{1z,new}}{2} \tag{3.21}$$

If first axle on the semi-trailer i.e, $axle_{21}$ is lifted then

$$A'_2 = A_2 + L_{22} + \left(\frac{L_{23}}{2}\right) \tag{3.22}$$

$$X'_2 = X_2 + L_{22} + \left(\frac{L_{23}}{2}\right) \tag{3.23}$$

$$F_{22z} = F_{23z} = \frac{F'_{1z,new}}{2} \tag{3.24}$$

If middle axle on the semi-trailer i.e, $axle_{22}$ is lifted then

$$A'_2 = A_2 + \left(\frac{L_{23}}{2}\right) \tag{3.25}$$

$$X'_2 = X_2 + \left(\frac{L_{22}}{2}\right) \tag{3.26}$$

$$F_{21z} = F_{23z} = \frac{F'_{1z,new}}{2} \tag{3.27}$$

Now equation 3.14 can be solved for F to get unknown vertical forces and coupling force of the tractor semi-trailer with any of the axles on the semi-trailer lifted. The new vertical forces is used as input parameter for the same vehicle combination and Low speed curve maneuvers is simulated to see the effect of lifted axles on the LSSP.

3.3 Implementation of Steered Axles in OpenPBS

The steps involved in adding the low speed steered axles for semi-trailers for the existing vehicle models in OpenPBS are as follows.

- Define a boolean parameter representing which axles of the vehicle are low speed steered. This Boolean parameter is added in basic vehicle parameter as shown in the below figure 3.8

```
parameter Boolean[nu,na] Lowspeed_Steered_axle=[false,false,false; false,false,true]
                         "True for each Steered axle";
```

Figure 3.8: Boolean Parameter for Low Speed Steered Axles

- Updating the equations so that the lateral force on the low speed steered axles becomes zero at low speeds. The slip angle α is set to zero on the low speed steered axles which in turn makes the the lateral force zero. Since modelica langauage is acausal modelling by setting $\alpha = 0$ in the below equation shown in figure 3.9 the steering angle delta (δ) on the low speed steered axles on semi-trailer is calculated explicitly as shown in figure 3.10. This part of semi-trailer steered axles is added in single track vehicle model.

```
/* Slip angles */
alpha = ((matrix(vy)*ones(1,na)+Lcog.*(matrix(wz)*ones(1,na)))./(matrix(vx)*ones(1,na))-delta);
```

Figure 3.9: Slip angle equation

```
for i in 1:nu loop
    for j in 1:na loop
        if i==1 and j==1 then
           delta[i,j] = delta_in;
        elseif Lowspeed_Steered_axle[i,j] == true and vx[1] <= 5 then
           alpha[i,j] = 0;
        else
           delta[i,j] = 0;
        end if;
      end for;
 end for;
```

Figure 3.10: To calculate steering angle on all steered axles except input steer on first axle

3.4 Implementation of Lifted Axles in OpenPBS

The steps involved in adding the lifted axles for semi-trailers for the existing vehicle models in OpenPBS for each transport mission.

- Permanently lifted axles for each transport mission can be implemented by directly using the vertical forces on non-lifted axles as input parameter to the models in OpenPBS by the user. As seen in the figure 3.11 the last axle of the semi-trailer is lifted and the same can be parameterized by setting the vertical force on axle to zero. However a methodology for calculating new vertical forces is provided in section 3.2 for permanently lifted axles for a tractor semi-trailer in OpenPBS.

```
Lifted_axle=[71607.3,82532.4,82532.4;63116,63116,0];
```

Figure 3.11: New vertical forces with one axle lifted

4

Case Study

4.1 Steered Axles

4.1.1 Steering Model on Tractor Semi-trailer Vehicle Combination With 2^{nd} & 3^{rd} Axle of Semi-trailer Steered

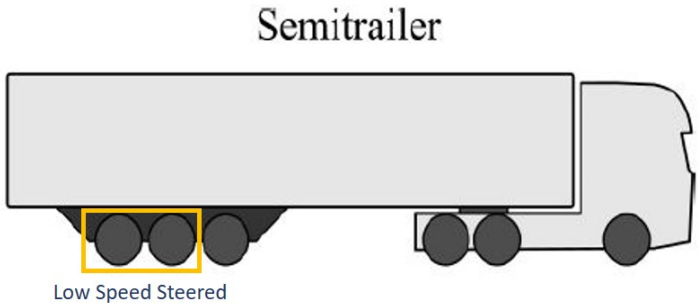

Figure 4.1: Tractor Semi-trailer Vehicle

This case study investigates two different steering models mentioned in methodology i.e, friction/zero side-slip steering model and algorithm based command steering for a tractor semi-trailer vehicle combination. The tractor semi-trailer vehicle combination consist of a 3-axle tractor and 3-axle semi-trailer.

The following three cases are considered to investigate the effect of semi-trailer steering on the LSSP of the vehicle combination.

- Friction/Zero side-slip steering model.
- Algorithm based command steering model with variable parameter a on tractor.
- Algorithm based command steering model with fixed parameter a on tractor.

Comparisons are made between Non-steered semi-trailer test case and steered cases for the same vehicle combination in terms of low speed swept path. The percentage improvement in swept path are also calculated to see the effect of different steering models individually with Non-steered as a reference. The results are presented and

the conclusions are made based on the result in the following results and discussion section.
All the above mentioned steering models were run for a low-speed curve maneuver defined with 90 and 180 degree of turn and radius of 12.5m in OpenPBS tool and the results are presented in the following section.

4.1.2 Steering Model on Nordic Vehicle Combination With 2^{nd} & 3^{rd} Axle of Semi-trailer Steered

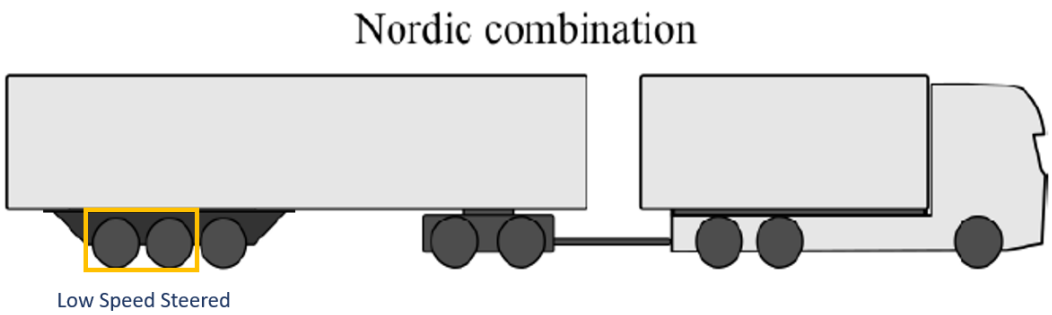

Figure 4.2: Nordic Vehicle Combination

This case study investigates two different steering models mentioned in methodology i.e, friction/zero side-slip steering model and algorithm based command steering for a tractor semi-trailer vehicle combination. The nordic vehicle combination consist of a 3-axle rigid truck, 2-axle dolly and a 3-axle semitrailer.

The following two cases are considered to investigate the effect of semi-trailer steering on the LSSP of the vehicle combination.

- Friction/Zero side-slip steering model .
- Algorithm based command steering model with variable parameter a on dolly.

The same comparisons are made as in the previous tractor- semitrailer case study and the conclusions are made based on the results in the following results and discussions section.
All the above mentioned steering models were run for a Low-speed curve maneuver defined with 90 and 180 degree of turn and radius of 12.5m in OpenPBS tool and the results are presented in the following section.

4.1.3 Steering Model on A-double Vehicle Combination With 2^{nd} & 3^{rd} Axle of 1^{st} Semi-trailer and 2^{nd} & 3^{rd} Axle of 2^{nd} Semi-trailer Steered Individually

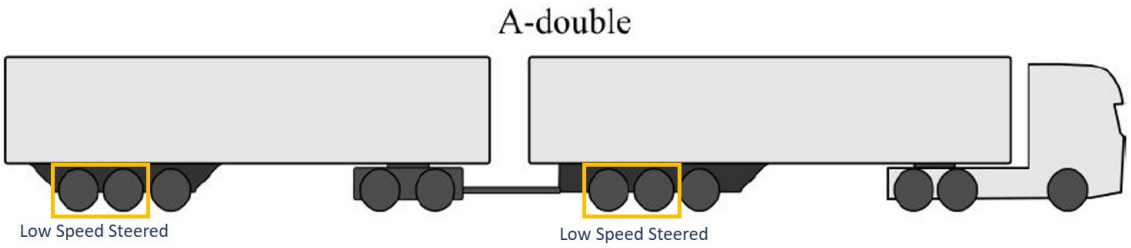

Figure 4.3: A-double Vehicle Combination

This case study investigates two different steering models mentioned in methodology i.e, friction/zero side-slip steering model and algorithm based command steering for a tractor semi-trailer vehicle combination. The A-double vehicle combination consist of a 3-axle tractor, 2-axle dolly and two 3-axle semi-trailers.

The following two cases are considered to investigate the effect of semi-trailer steering on the LSSP of the vehicle combination.

- Friction/Zero side-slip steering model .
- Algorithm based command steering model with variable parameter a on tractor.
- Algorithm based command steering model with variable parameter a on dolly.

Since A-double vehicle combination has two semi-trailers which allows to have a steering model on any of the semi-trailer individually and the same comparisons are made as in the previous tractor semi-trailer case study and the conclusions are made based on the results in the following results and discussions section.
All the above mentioned steering models were run for a Low-speed curve maneuver defined with 90 and 180 degree of turn and radius of 12.5m in OpenPBS tool and the results are presented in the following section.

4.1.4 Steering Model on A-double Vehicle Combination With All Axles Steered Individually

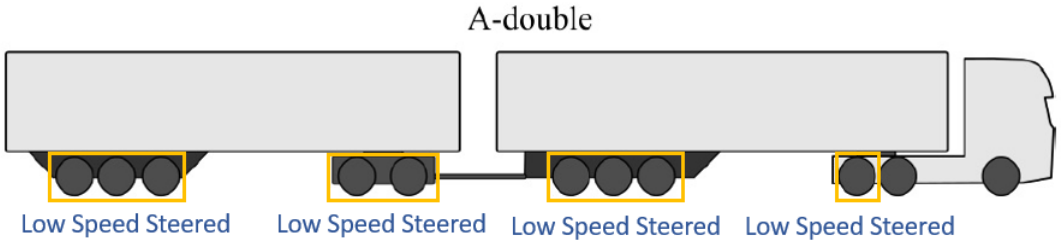

Figure 4.4: A-double Vehicle Combination Multi Axles Steered

This case study investigates only one of the steering model mentioned in methodology i.e, friction/zero side-slip steering model for a A-double vehicle combination. The A-double vehicle combination consist of a 3-axle tractor, 2-axle dolly and two 3-axle semi-trailers.

The following test case is considered to investigate the effect of low speed semi-trailer steering on LSSP of the vehicle combination. As highlighted in the figure 4.4 each axle is low speed steered individually and the low speed swept path is recorded.

- Friction/Zero side-slip steering model.

Friction/Zero side-slip steering model was simulated for a Low-speed curve maneuver defined with 90 and 180 degree of turn and radius of 12.5m in OpenPBS tool and the results are presented in the following section.

4.2 Lifted Axles

4.2.1 Lifted Axles on Tractor Semi-trailer Vehicle Combination with 1^{st}, 2^{nd} & 3^{rd} axles lifted individually

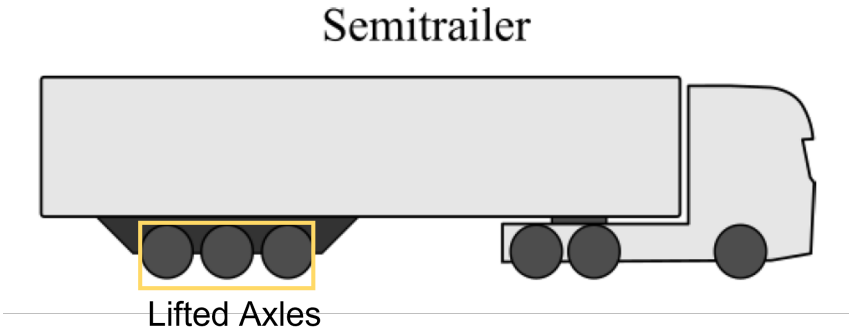

Figure 4.5: Tractor Semi-trailer Vehicle

This case study investigates the effect of lifted axles on the LSSP of the vehicle combination during a low speed curve maneuver. Tractor semi-trailer vehicle combination which consist of a 3-axle tractor and 3-axle semi-trailer is considered. Each axle of the semi-trailer is considered to be lifted at low speeds. Three different cases are considered to see the effect of LSSP when any of the axle is defined to be lifted.

- First semi-trailer axle lifted
- Second semi-trailer axle lifted
- Last semi-trailer axle lifted

The results for LSSP is compared with non lifted axle.

5

Results and Discussion

5.1 Steered Axle Results and Discussion

5.1.1 Results for Steering Models on Tractor Semi-trailer Vehicle Combination with 2^{nd} & 3^{rd} Axle of Semi-trailer Steered

5.1.1.1 Results: Low speed turn of 90 degree and 12.5 m radius for friction-zero side-slip steer, algorithm based command steer with variable parameter a, algorithm based command steer with constant parameter a

when in a corner the algorithm based command steering method steers two of the trailer axles to reduce the effective wheelbase of the trailer to that of the equivalent single defined by cebon et al in his study [20]. The zero side-slip point is calculated only on the leading unit and Since both 2^{nd} & 3^{rd} axle of the semi trailer are steered together the zero side-slip point on the trailing unit is considered on the first trailer axle.

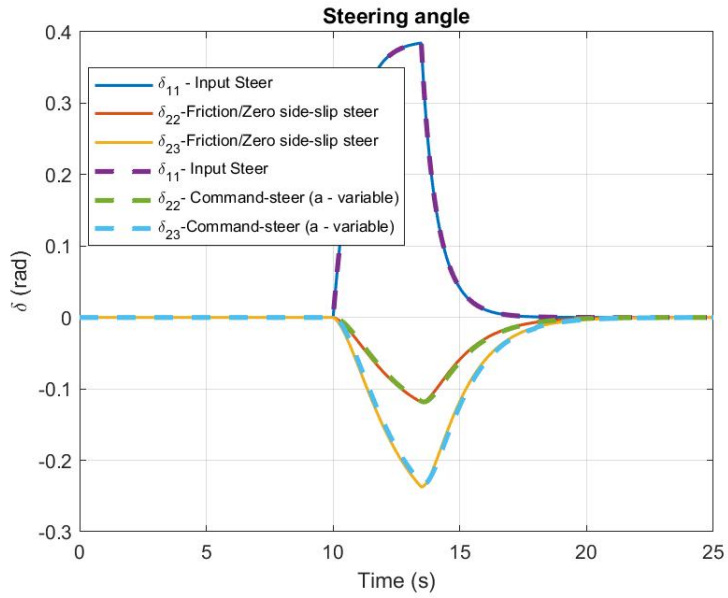

Figure 5.1: Tractor semi-trailer :- steering angle for 90 degree turn & 12.5m radius.

The figure 5.1 is the steering angles on the first axle (δ_{11}) and the two semi-trailer axles (δ_{22} & δ_{23}) that are selected to be steered. The steering angles (δ_{22} & δ_{23}) represent the friction steered and algorithm based command steered with variable parameter 'a' models.

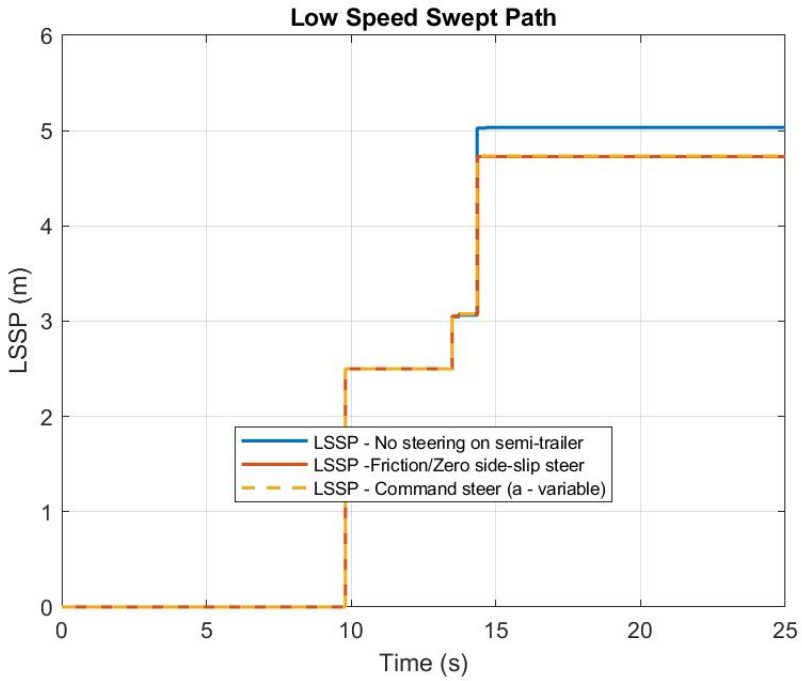

Figure 5.2: Tractor Semi-trailer :- Low Speed Swept Path for 90 degree & 12.5m radius

The figure 5.2 shows the swept path of the selected vehicle combination from start to end for a defined manoeuvre. It includes the measure of low speed swept path for three different cases for the same vehicle combination. The first case being the non steered axles on semi-trailer and the other two cases with two steered axles ($axle_{22}$ & $axle_{23}$) on semi-trailer for friction-zero side-slip steering and algorithm based command steering with variable parameter 'a' models.

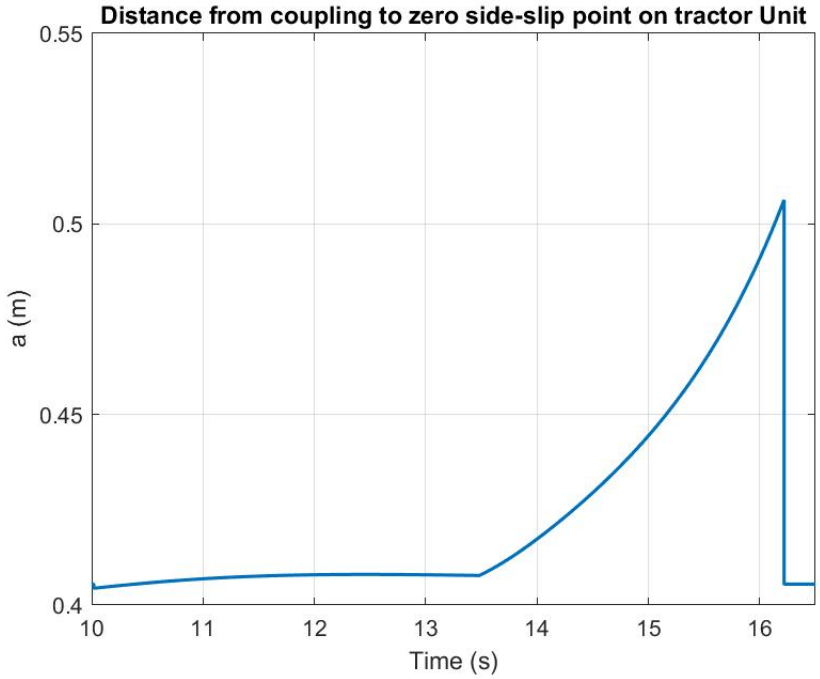

Figure 5.3: Tractor semi-trailer :- Distance from coupling to the zero side-slip point (a) on leading unit for 90 degree & 12.5m radius

The parameter 'a' which is the distance measure from the fifth wheel coupling and the zero side slip point on the tractor unit is plotted in the figure 5.3.

The individual swept paths are tabulated and compared in table 5.1 below.

	LSSP (m)
Non-Steered	5.03
friction-zero side-slip Steered	4.72
Algorithm Based Command Steered With Variable Parameter a	4.73

Table 5.1: Tractor semi-trailer :- low speed swept path for 90 degree & 12.5m radius

The percentage improvement in swept path for friction-zero side-slip steered and algorithm based command steered compared to non steered case are calculated and tabulated in the table 5.2.

	Percentage improvement in LSSP (%)
Non-Steered and friction-zero side-slip steered	6.16
Non-Steered and Algorithm Based Command Steered With Variable Parameter a	6.20

Table 5.2: Tractor semi-trailer :- percentage improvement in low speed swept path for 90 degree & 12.5m radius

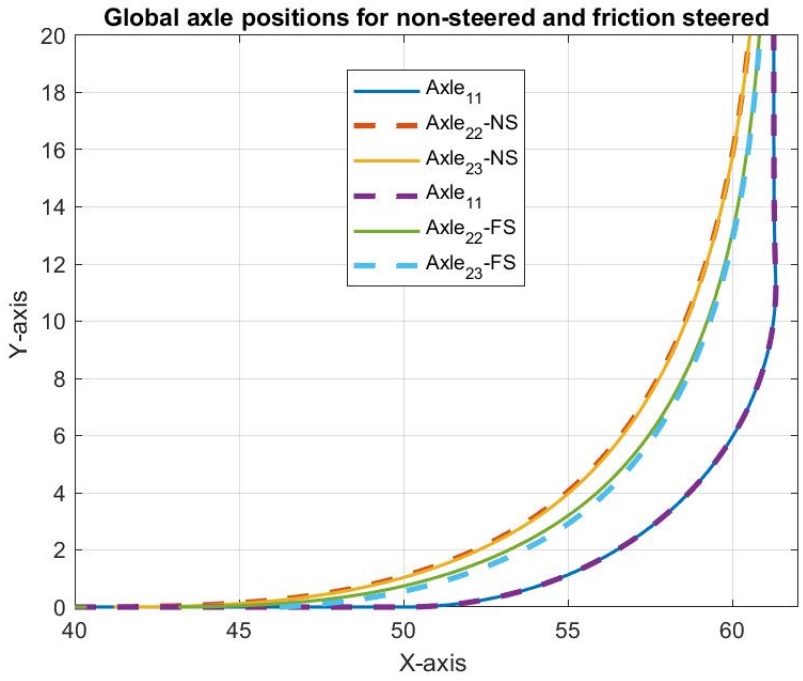

Figure 5.4: Tractor semi-trailer :- axle global position - friction steered (FS) and non-steered (NS) case for 90 degree & 12.5m radius

The figure 5.4 represents the axle position/trajectory along the path of the maneuver for non-steered and friction-zero side-side slip steering model and it is evident that non-steered axle trace a different trajectory compared to the friction steered axles there by reducing the swept path during the corner.

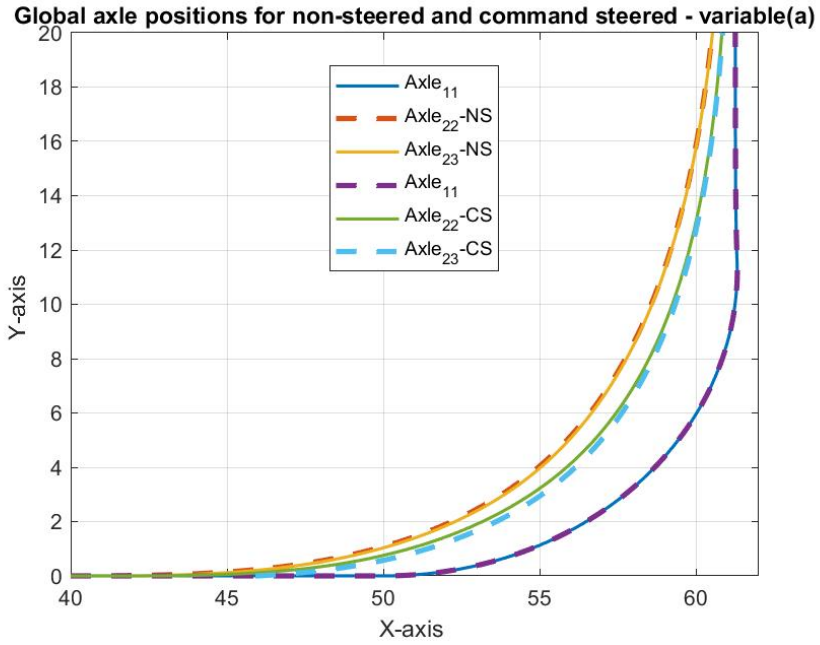

Figure 5.5: Tractor semi-trailer :- axle global position - command steered (CS) and non-steered (NS) case for 90 degree & 12.5m radius

The figure 5.5 represents the axle position/trajectory along the path of the maneuver for non-steered and command steering model and it also evident that non-steered axle traces a different trajectory compared to the command steered axles which in turn reduces the swept path during the corner.

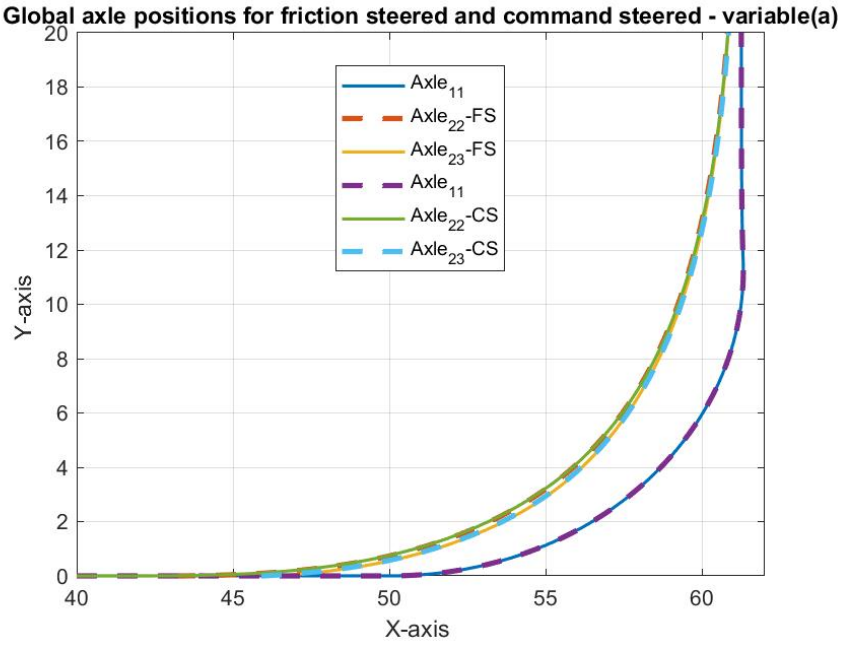

Figure 5.6: Tractor semi-trailer :- axle global position - command steered (CS) and friction steered (FS) case for 90 degree & 12.5m radius

The figure 5.6 represents the axle position/trajectory along the path of the maneuver for friction steering and command steering model. It can be concluded that friction steer and command steer are close to each other which also reflects in percentage improvement of LSSP from the table 5.2.

The observation from the figure 5.3 concludes that distance from the fifth wheel coupling to the zero side slip point is not constant. The same test case was considered with few constant values for the parameter 'a' on either side of the coupling point to see the effect of algorithm based command steer to different constant parameter'a' values.
The low speed swept path for each constant 'a' values in the table **??** are recorded for algorithm based command steer. The swept path for each case is tabulated in 5.3.

The parameter a (m) with constant positive values	**LSSP (m) for command steer**	**The parameter a (m) with constant negative values**	**LSSP (m) for command steer**
0.2	4.73	-0.2	4.74
0.4	4.72	-0.4	4.75
0.6	4.71	-0.6	4.76
0.8	4.7	-0.8	4.77
1	4.69	-1	4.78
1.2	4.68	-1.2	4.79
1.5	4.66	-1.5	4.8

Table 5.3: Tractor semi-trailer :- LSSP for constant a values for 90 degree & 12.5 m radius

The parameter a (m) with constant positive values	**Percentage improvement of LSSP for command steer compared to non-steered**	**The parameter a (m) with constant negative values**	**Percentage improvement of LSSP for command steer compared to non-steered**
0.2	5.96 %	-0.2	5.76 %
0.4	6.16 %	-0.4	5.56 %
0.6	6.36 %	-0.6	5.36 %
0.8	6.56 %	-0.8	5.16 %
1	6.75 %	-1	4.97 %
1.2	6.95 %	-1.2	4.77 %
1.5	7.35 %	-1.5	4.57 %

Table 5.4: Tractor semi-trailer :- percentage improvement of LSSP for command steer with constant values for parameter 'a' for 90 degree & 12.5 m radius

The percentage improvement of LSSP for algorithm based command steered compared to non-steered with different constant values of a are tabulated in 5.4

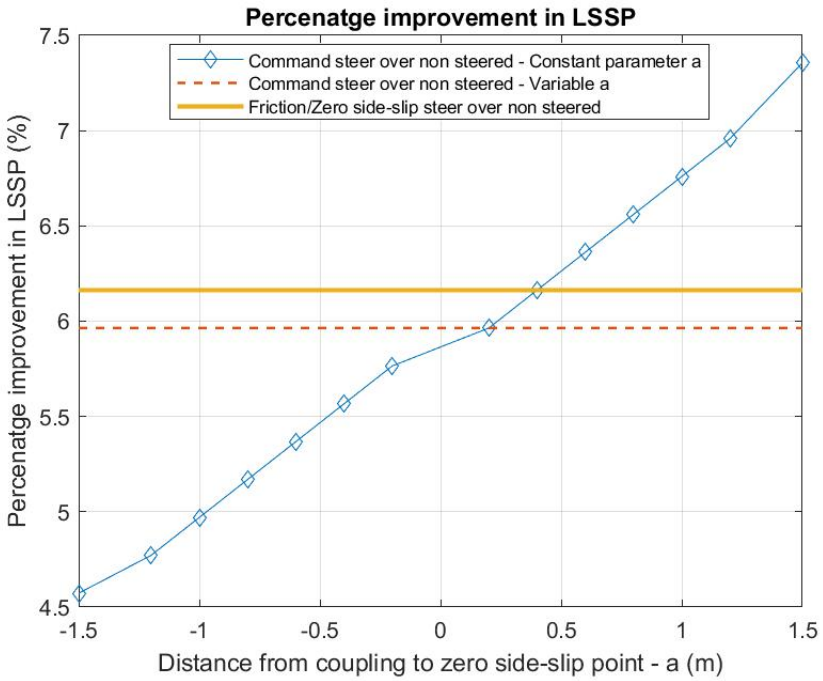

Figure 5.7: Percentage improvement in LSSP for 90 degree & 12.5 m radius

In the figure 5.7 the red dashed line is the percentage improvement of LSSP for command steered with variable parameter a compared to non-steered and the orange solid line is the percentage improvement of LSSP for friction-zero side-slip steer compared to non-steered.
The figure also shows the percentage improvement of LSSP for command steered with constant values of parameter a compared to non-steered axles as mentioned in the table 5.4. The position of the zero side-slip point towards the $axle_{13}$ & $axle_{11}$ is considered as positive and negative respectively with coupling position fixed. The different distance values between the coupling point and the zero side-slip point that are considered are in table 5.3. As the position of the zero side-slip point moves towards the $axle_{13}$ and $axle_{12}$ the distance from coupling increases on either side respectively.

It is also evident from figure 5.7 that if the distance of zero side-slip point is increased from coupling towards the $axle_{13}$ the percentage improvement also increases and if the distance of zero side-slip point is increased from coupling towards the $axle_{12}$ the percentage improvement also decreases. Command steer with constant parameter 'a' can be used to achieve even more better swept path at low speeds while compromising more tyre ware.

The percentage difference between the friction-zero side-slip steer and command steer compared to non-steered case is because in friction-zero side-slip steer the lat-

eral force on the axle is set to zero while command steer also assumes the zero side-slip yet it steer in relation to articulation point and there exist minimal lateral forces due to which there is a small difference in percentage improvement.

5.1.1.2 Results:- Low speed turn of 180 degree and 12.5 m radius for friction-zero side-slip steer and algorithm based command steer with variable parameter a

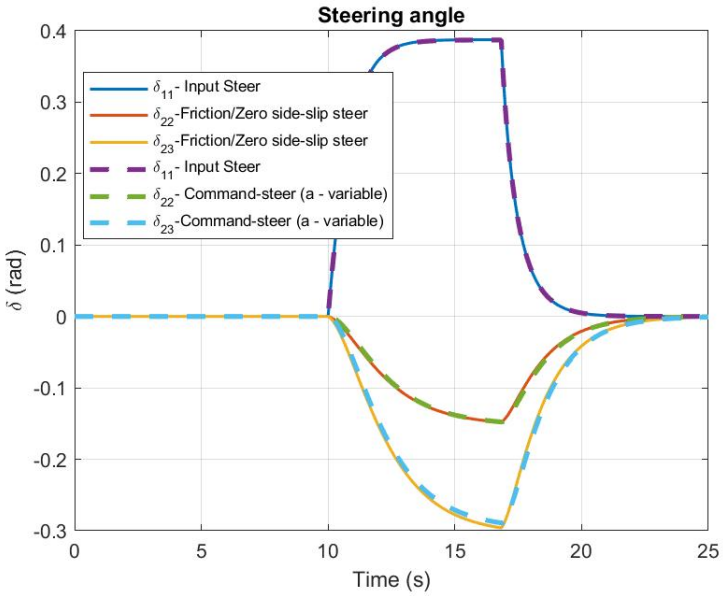

Figure 5.8: Tractor semi-trailer :- Steering Angle for 180 degree & 12.5m radius

The figure 5.8 is the steering angles on the first axle (δ_{11}) and the two semi-trailer axles (δ_{22} & δ_{23}) that are selected to be steered. The steering angles (δ_{22} & δ_{23}) represent the friction steered and algorithm based command steered with variable parameter 'a' models.

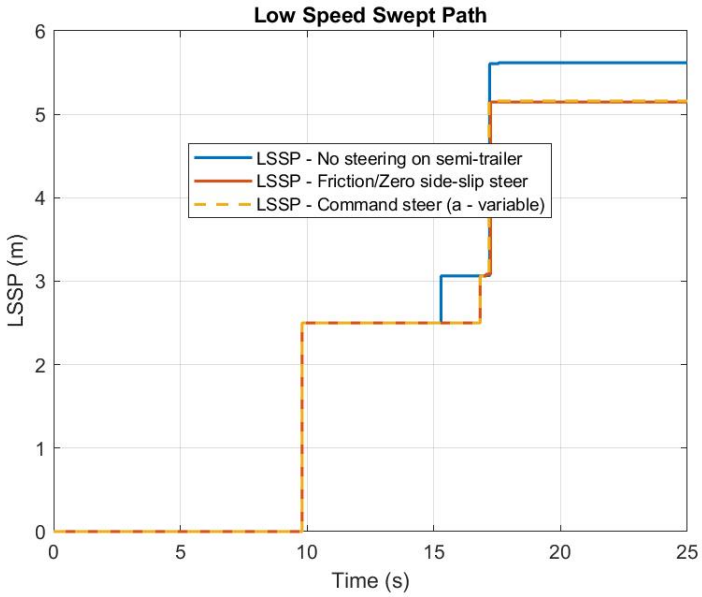

Figure 5.9: Tractor semi-trailer :- low speed swept path for 180 degree & 12.5m radius

The figure 5.9 shows the swept path of the selected vehicle combination from start to end for a defined manoeuvre. It includes the measure of low speed swept path for three different cases for the same vehicle combination. The first case being the non steered axles on semi-trailer and the other two cases with two steered axles ($axle_{22}$ & $axle_{23}$) on semi-trailer for friction-zero side-slip steering and algorithm based command steering with variable parameter 'a' models.

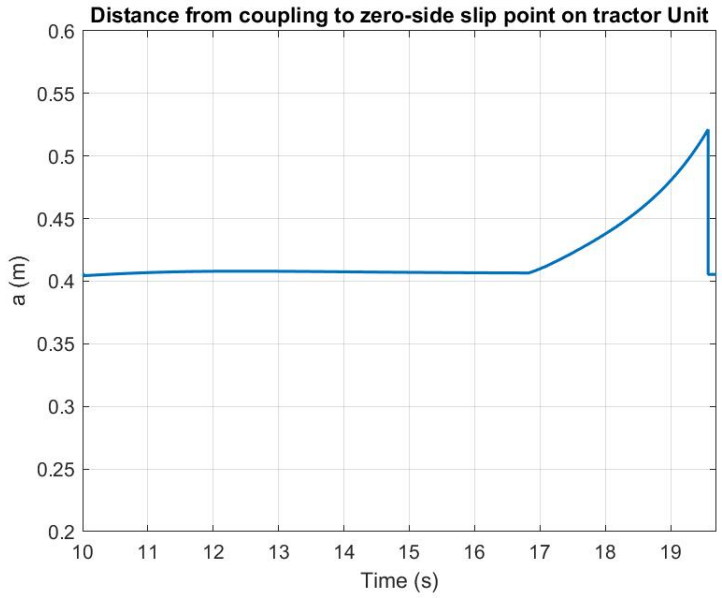

Figure 5.10: Tractor semi-trailer :- Distance from coupling to the zero side-slip point (a) on leading unit for 180 degree & 12.5m radius

The parameter 'a' which is the distance measure from the fifth wheel coupling and the zero side-slip point on the tractor unit is plotted in the figure 5.10.
The individual swept paths are tabulated and compared in table 5.5 below. From the same table it is clear that the non-steered case has the highest swept path compared to the other two semi-trailer steered cases and it can be concluded that if the axles of the trailer are steered it possible to achieve a better swept path compared to non-steered case.

	LSSP (m)
Non-Steered	5.61
friction-zero side-slip Steered	5.14
Algorithm Based Command Steered With Variable Parameter a	5.15

Table 5.5: Tractor semi-trailer :- low speed swept path for three different concept of low speed steered axles for 180 degree & 12.5m radius

The percentage improvement in swept path for friction-zero side-slip steered and algorithm based command steered compared to non steered case are calculated and tabulated in the table 5.6.

	Percentage improvement in LSSP (%)
Non-Steered and friction-zero side-slip steered	8.37
Non-Steered and Algorithm Based Command Steered With Variable Parameter a	8.2

Table 5.6: Tractor semi-trailer :- percentage improvement in low speed swept path for 180 degree & 12.5m radius

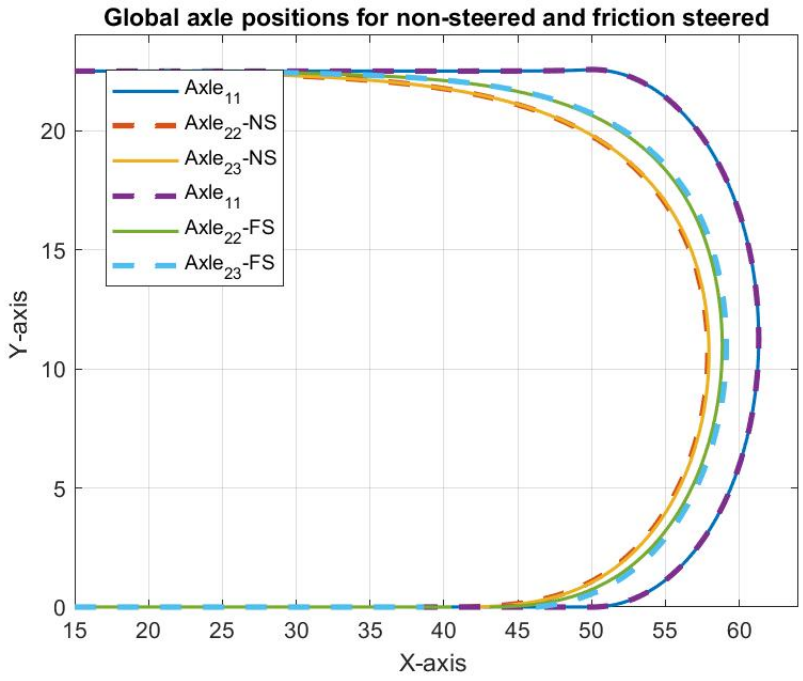

Figure 5.11: Tractor Semi-trailer :- axle global position - friction steered (FS) and non-steered (NS) case for 180 degree & 12.5m radius

The figure 5.11 represents the axle position/trajectory along the path of the maneuver for non-steered and friction-zero side-side slip steering model and it is evident that non-steered axle trace a different trajectory compared to the friction steered axles there by reducing the swept path during the corner.

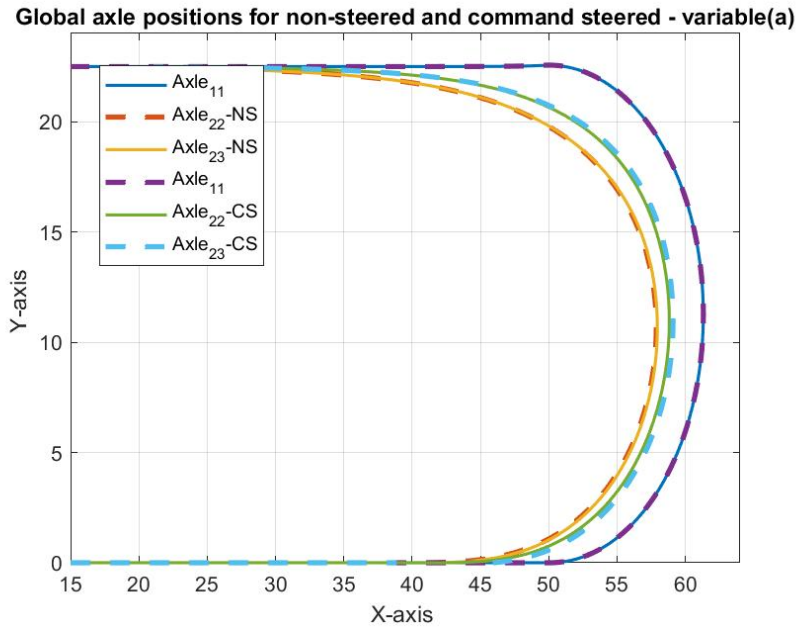

Figure 5.12: Tractor semi-trailer :- axle global position - command Steered (CS) and Non-steered (NS) case for 180 degree & 12.5m radius

The figure 5.12 represents the axle position/trajectory along the path of the maneuver for non-steered and command steering model and it also evident that non-steered axle traces a different trajectory compared to the command steered axles which in turn reduces the swept path during the corner.

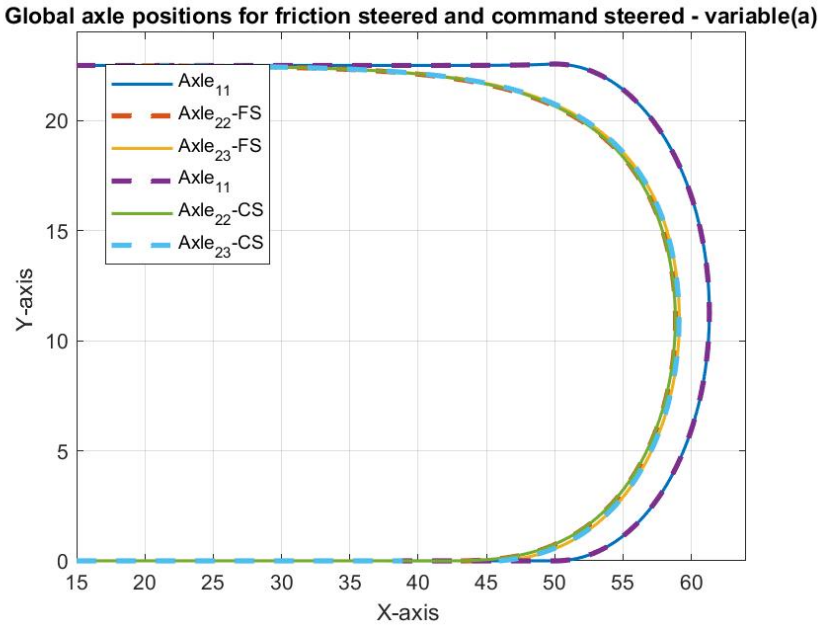

Figure 5.13: Tractor semi-trailer :- axle global position - Friction Steered (FS) and Command Steered (CS) case for 180 degree & 12.5m radius

The figure 5.13 represents the axle position/trajectory along the path of the maneuver for friction steering and command steering model. It can be concluded that friction steer and command steer are close to each other which also reflects in percentage improvement of LSSP from the table 5.6.

The observation from the figure 5.10 concludes that distance from the fifth wheel coupling to the zero side slip point is not constant.
The low speed swept path for each constant 'a' values in the table 5.7 are recorded for algorithm based command steer.

The parameter a (m) with constant positive values	**LSSP (m) for command steer**	**The parameter a (m) with constant negative values**	**LSSP (m) for command steer**
0.2	5.16	-0.2	5.19
0.4	5.15	-0.4	5.20
0.6	5.13	-0.6	5.21
0.8	5.11	-0.8	5.22
1	5.09	-1	5.24
1.2	5.07	-1.2	5.25
1.5	5.04	-1.5	5.26

Table 5.7: Tractor semi-trailer :- LSSP for constant a values for 180 degree & 12.5 m radius

The percentage improvement of LSSP for algorithm based command steered compared to non-steered with different constant values of a are tabulated in the table 5.8

The parameter a (m) with constant positive values	**Percentage improvement of LSSP for command steer compared to non-steered**	**The parameter a (m) with constant negative values**	**Percentage dis-improvement of LSSP for command steer compared to non-steered**
0.2	8.02 %	-0.2	7.30 %
0.4	8.19 %	-0.4	7.3 %
0.6	8.55 %	-0.6	7.13 %
0.8	8.91 %	-0.8	6.95 %
1	9.26 %	-1	6.59 %
1.2	9.62 %	-1.2	6.41 %
1.5	10.16 %	-1.5	6.23 %

Table 5.8: Tractor semi-trailer :- percentage improvement of LSSP for command steer with constant values for parameter 'a' for 180 degree & 12.5 m radius

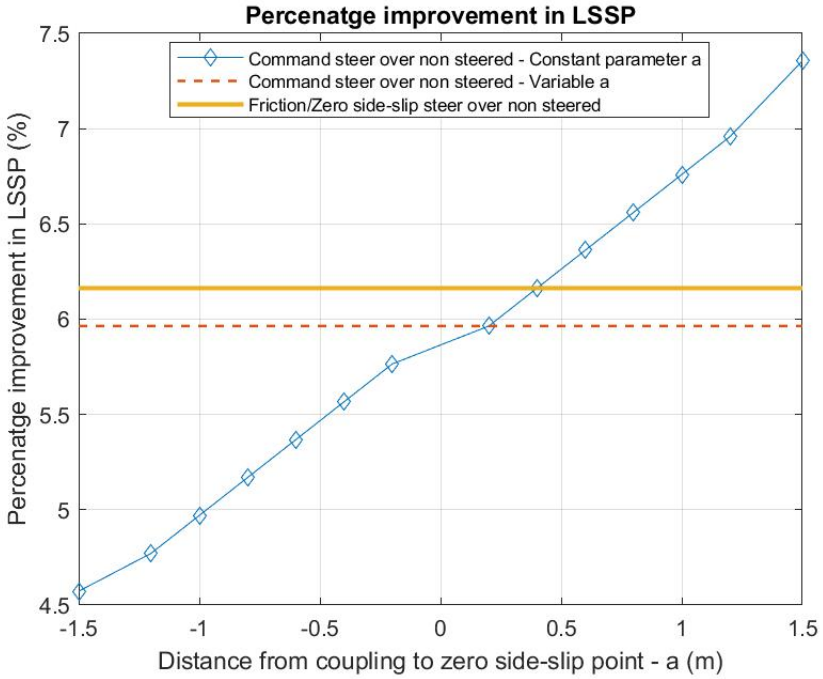

Figure 5.14: Percentage improvement in LSSP for 180 deg & 12.5m radius

In the figure 5.14 the red dashed line is the percentage improvement of LSSP for command steered with variable parameter a compared to non-steered. The orange solid line is the percentage improvement of LSSP for friction-zero side-slip steer compared to non-steered axles.
The figure also shows the percentage improvement of LSSP for command steered with constant values of parameter a compared to non-steered as mentioned in the table 5.8. The position of the zero side-slip point towards the $axle_{13}$ & $axle_{11}$ is considered as positive and negative respectively with coupling position fixed. The different distance values between the coupling point and the zero side-slip point considered are in table 5.7. As the position of the zero side-slip point moves towards the $axle_{13}$ and $axle_{12}$ the distance from coupling increases on either side respectively and the trend of the graph looks similar to the 90 degree and 12.5 m radius.

5.1.2 Results For Steering Models on Nordic Vehicle Combination With 2^{nd} & 3^{rd} Axle of Semi-trailer Steered

5.1.2.1 Results:- Low speed turn of 90 degree and 12.5 m radius for friction-zero side-slip steer and algorithm based command steer with variable parameter a

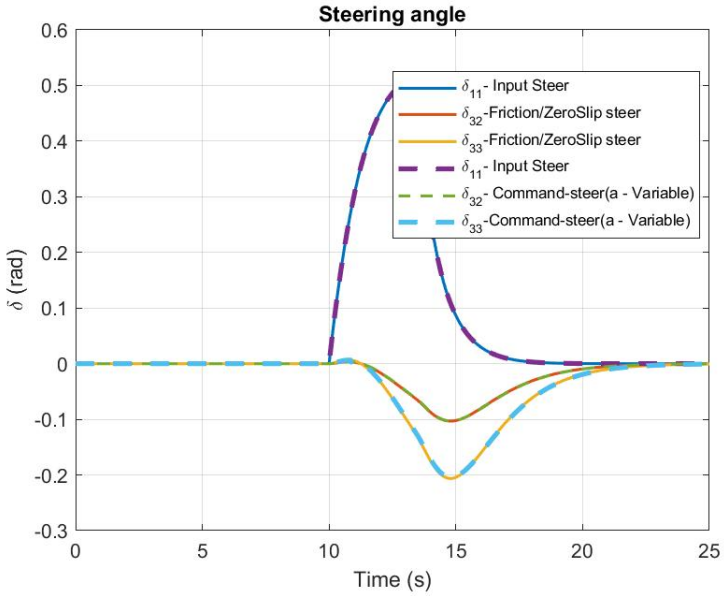

Figure 5.15: Nordic combination :- steering angle for 90 degree & 12.5m radius

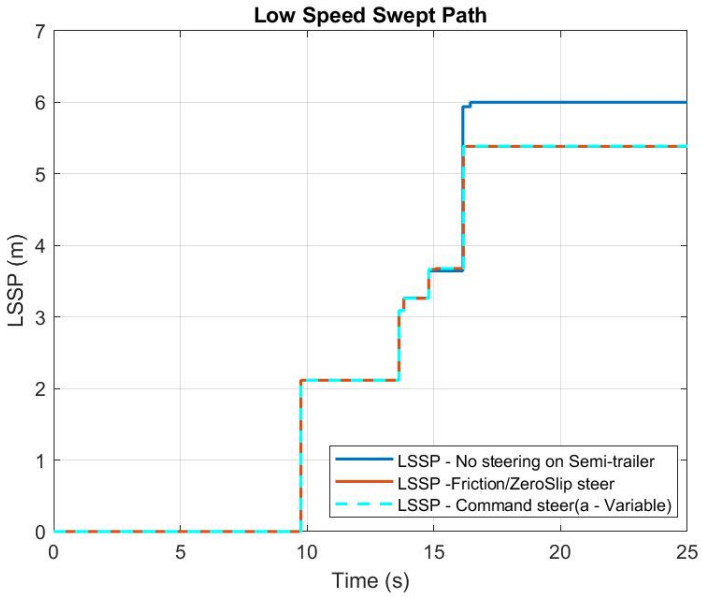

Figure 5.16: Nordic combination :- Low Speed Swept Path for 90 degree & 12.5m radius

The figure 5.15 is the steering angles on the first axle (δ_{11}) and the two semi-trailer axles (δ_{32} & δ_{33}) that are selected to be steered. The steering angles (δ_{32} & δ_{33}) represent the friction steered and algorithm based command steered with variable parameter 'a' models.

The figure 5.16 shows the swept path of the selected vehicle combination from start to end for a defined manoeuvre. It includes the measure of low speed swept path for three different cases for the same vehicle combination. The first case being the non steered axles on semi-trailer and the other two cases with two steered axles ($axle_{32}$ & $axle_{33}$) on semi-trailer for friction-zero side-slip steering and algorithm based command steering with variable parameter 'a' models.

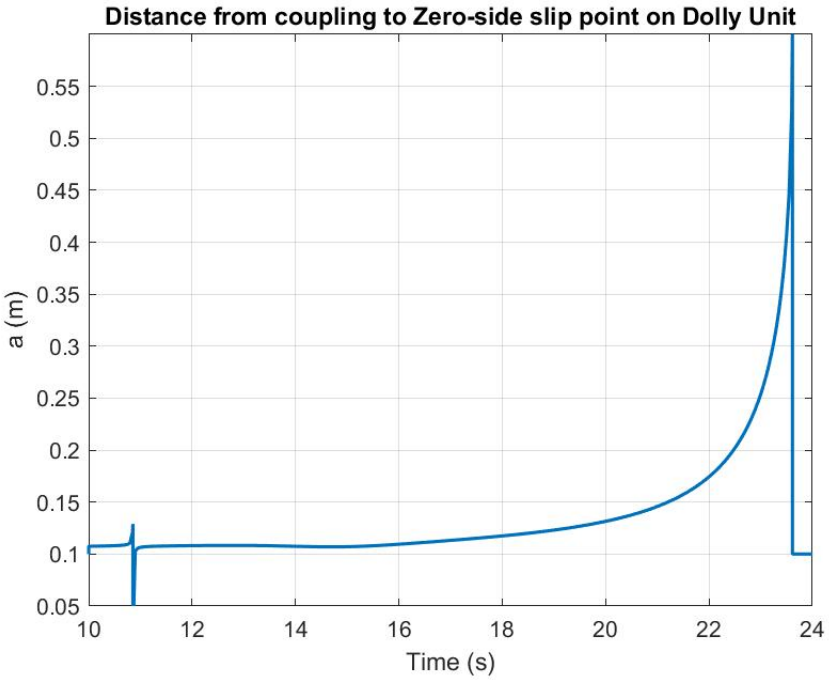

Figure 5.17: Nordic combination :- distance from coupling to the zero side-slip point (a) on leading unit for 90 degree & 12.5m radius

The parameter 'a' which is the distance measure from the fifth wheel coupling and the zero side slip point on the tractor unit is plotted in the figure 5.17.

The individual swept paths are tabulated and compared in table 5.9 below. From the same table it is clear that the non-steered case has the highest swept path compared to the other two semi-trailer steered cases and it can be concluded that if the axles of the trailer are steered it possible to achieve a better swept path compared to non-steered case.

	LSSP (m)
Non-Steered	6.01
friction-zero side-slip Steered	5.38
Algorithm Based Command Steered With Variable Parameter a	5.38

Table 5.9: Nordic combination :- low speed swept path for three different concept of low speed steered axles for 90 degree & 12.5m radius

The percentage improvement in swept path for friction-zero side-slip steered and algorithm based command steered compared to non steered case are calculated and tabulated in the table 5.10.

	Percentage improvement in LSSP (%)
Non-Steered and friction-zero side-slip steered	10.48
Non-Steered and Algorithm Based Command Steered With Variable Parameter a	10.48

Table 5.10: Nordic combination :- percentage improvement in low speed swept path for 90 degree & 12.5m radius

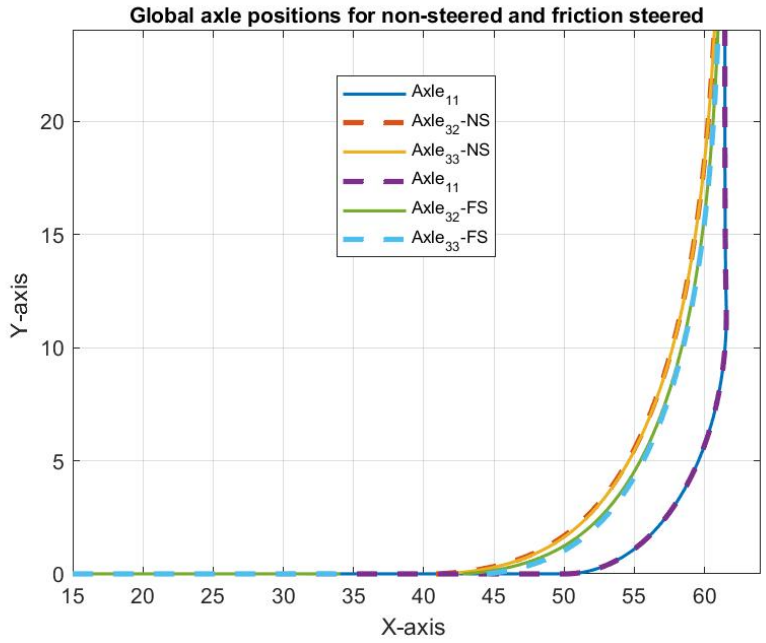

Figure 5.18: Axle global position :- friction steered (FS) and non-steered (NS) case for 90 degree & 12.5m radius

The figure 5.18 represents the axle position/trajectory along the path of the maneuver for non-steered and friction-zero side-side slip steering model and it is evident

that non-steered axle trace a different trajectory compared to the friction steered axles there by reducing the swept path during the corner.

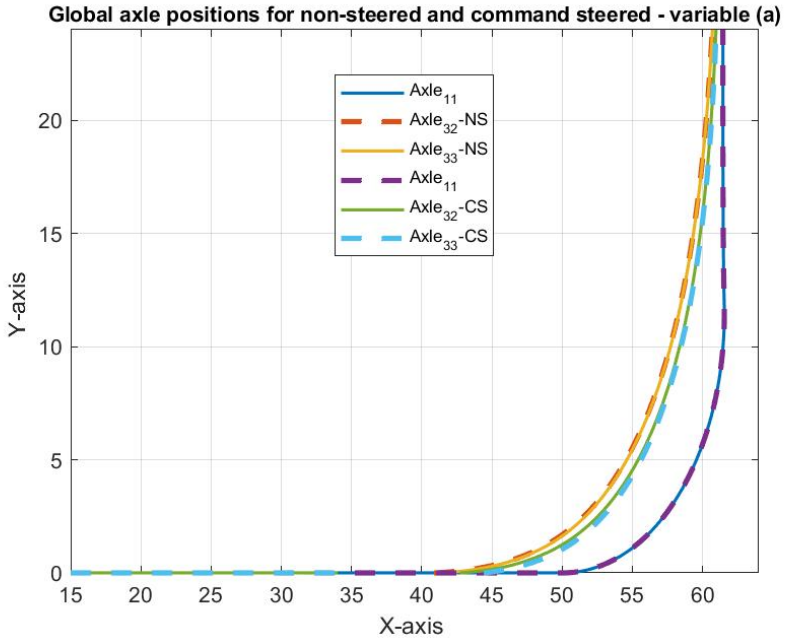

Figure 5.19: Axle global position :- command steered (CS) and non-steered (NS) case for 90 degree & 12.5m radius

The figure 5.19 represents the axle position/trajectory along the path of the maneuver for non-steered and command steering model and it also evident that non-steered axle traces a different trajectory compared to the command steered axles which in turn reduces the swept path during the corner.

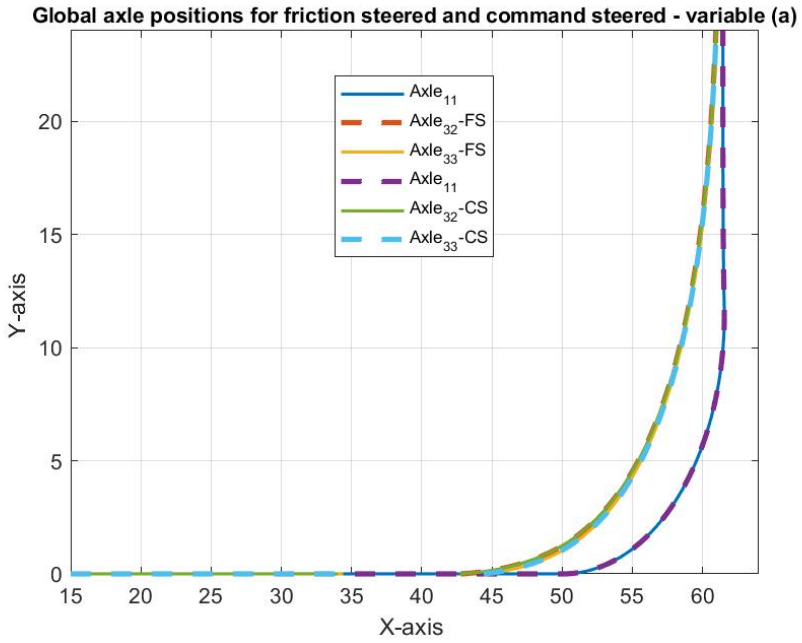

Figure 5.20: Axle global position :- command steered (CS) and friction steered (FS) case for 90 degree & 12.5m radius

The figure 5.20 represents the axle position/trajectory along the path of the maneuver for friction steering and command steering model. It can be concluded that friction steer and command steer are close to each other which also reflects in percentage improvement of LSSP from the table 5.10.

5.1.2.2 Results:- Low speed turn of 180 degrees and 12.5 m radius for friction-zero side slip steer and algorithm based command steer with variable parameter a

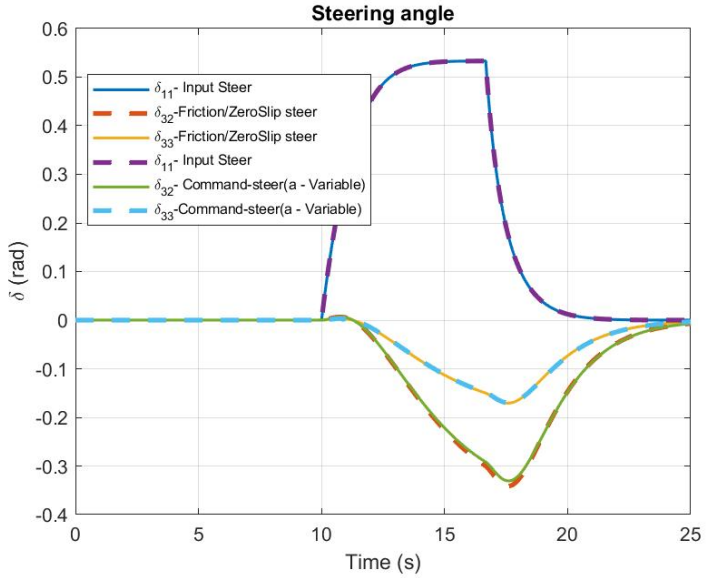

Figure 5.21: Nordic combination :- steering angle for 180 degree & 12.5m radius

The figure 5.15 is the steering angles on the first axle (δ_{11}) and the two semi-trailer axles (δ_{32} & δ_{33}) that are selected to be steered. The steering angles (δ_{32} & δ_{33}) represent the friction steered and algorithm based command steered with variable parameter 'a' models.

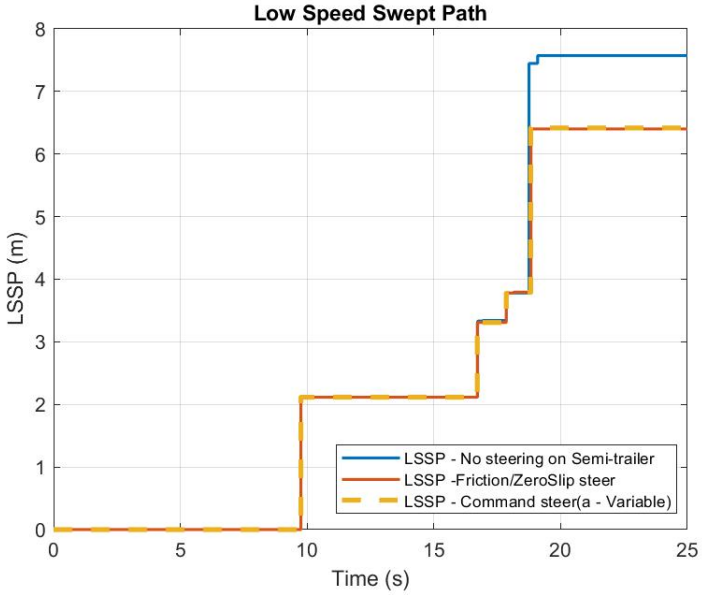

Figure 5.22: Nordic combination :- low speed swept path for 180 degree & 12.5m radius

The figure 5.22 shows the swept path of the selected vehicle combination from start to end for a defined manoeuvre. It includes the measure of low speed swept path for three different cases for the same vehicle combination. The first case being the non steered axles on semi-trailer and the other two cases with two steered axles ($axle_{32}$ & $axle_{33}$) on semi-trailer for friction-zero side-slip steering and algorithm based command steering with variable parameter 'a' models.

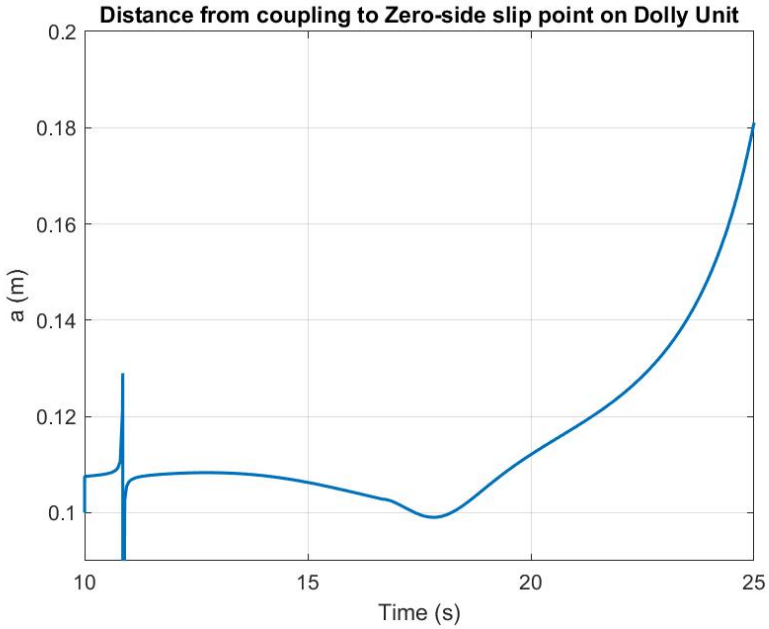

Figure 5.23: Nordic combination :- distance from coupling to the zero side-slip point (a) on leading unit for 180 degree & 12.5m radius

The parameter 'a' which is the distance measure from the fifth wheel coupling and the zero side slip point on the tractor unit is plotted in the figure 5.23.

The individual swept paths are tabulated and compared in table 5.11 below. From the same table it is clear that the non-steered case has the highest swept path compared to the other two semi-trailer steered cases and it can be concluded that if the axles of the trailer are steered it possible to achieve a better swept path compared to non-steered case.

	LSSP (m)
Non-Steered	7.57
friction-zero Side-slip Steered	6.40
Algorithm Based Command Steered With Variable Parameter a	6.41

Table 5.11: Nordic combination :- low speed swept path for three different concept of low speed steered axles for 180 degree & 12.5m radius

The percentage improvement in swept path for friction-zero side-slip steered and

algorithm based command steered compared to non steered case are calculated and tabulated in the table 5.12.

	Percentage improvement in LSSP (%)
Non-Steered and friction-zero Side-slip steered	15.45
Non-Steered and Algorithm Based Command Steered With Variable Parameter a	15.45

Table 5.12: Nordic combination :- percentage improvement in low speed swept path for 180 degree & 12.5m radius

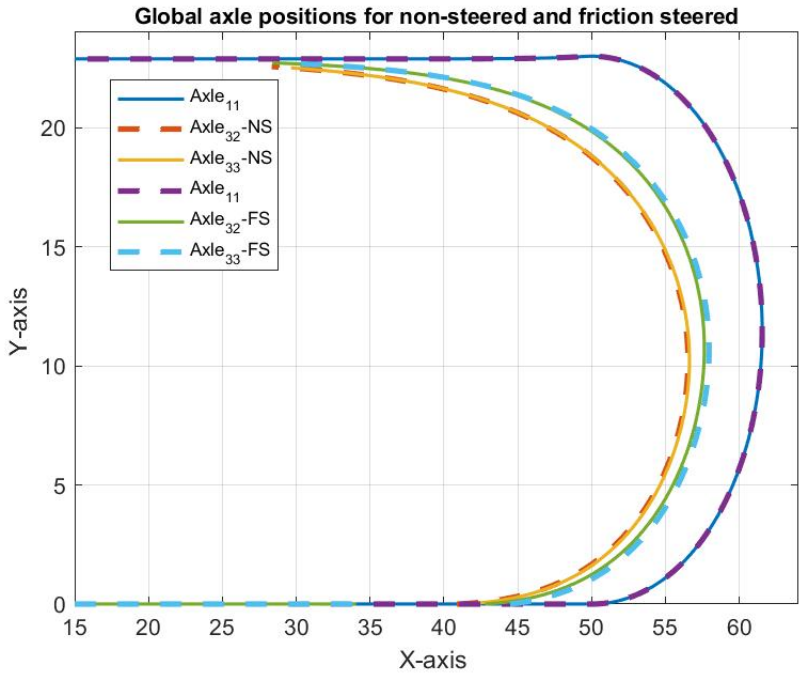

Figure 5.24: Axle global position :- Friction steer (FS) and non-steered (NS) for 180 degree & 12.5m radius

The figure 5.24 represents the axle position/trajectory along the path of the maneuver for non-steered and friction-zero side-side slip steering model and it is evident that non-steered axle trace a different trajectory compared to the friction steered axles there by reducing the swept path during the corner.

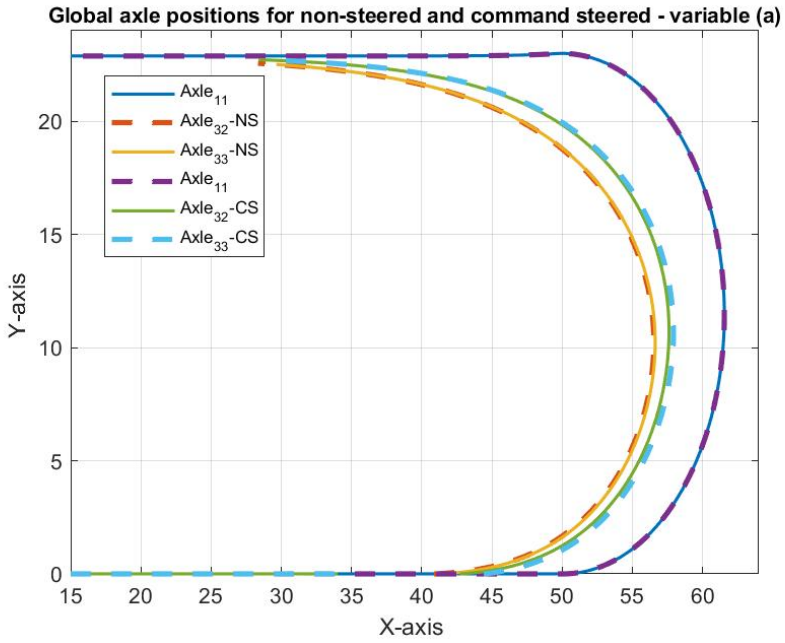

Figure 5.25: Axle global position :- command steer (CS) and non-steered (NS) for 180 degree & 12.5m radius

The figure 5.25 represents the axle position/trajectory along the path of the maneuver for non-steered and command steering model and it also evident that non-steered axle traces a different trajectory compared to the command steered axles which in turn reduces the swept path during the corner.

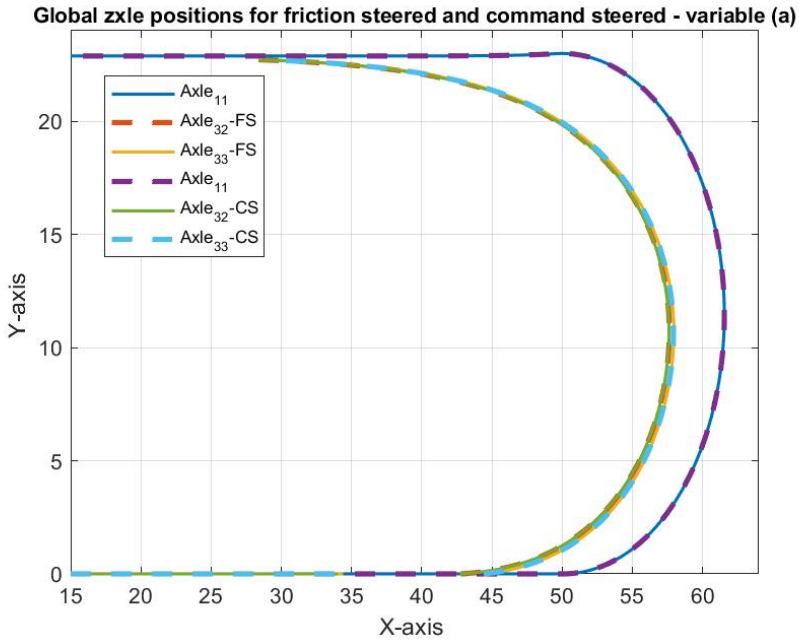

Figure 5.26: Axle global position :- command steer (CS) and friction steered (FS) for 180 degree & 12.5m radius

The figure 5.26 represents the axle position/trajectory along the path of the maneuver for friction steering and command steering model. It can be concluded that friction steer and command steer are close to each other which also reflects in percentage improvement of LSSP from the table 5.12.

5.1.3 Results For Steering Models on A-double Vehicle Combination With 2^{nd} & 3^{rd} Axle of 1^{st} Semi-trailer and 2^{nd} & 3^{rd} Axle of 2^{nd} Semi-trailer Steered Individually

5.1.3.1 Results:- Low speed turn of 90 degree and 12.5 m radius for friction-zero side-slip steer and algorithm based command steer with variable parameter a

.

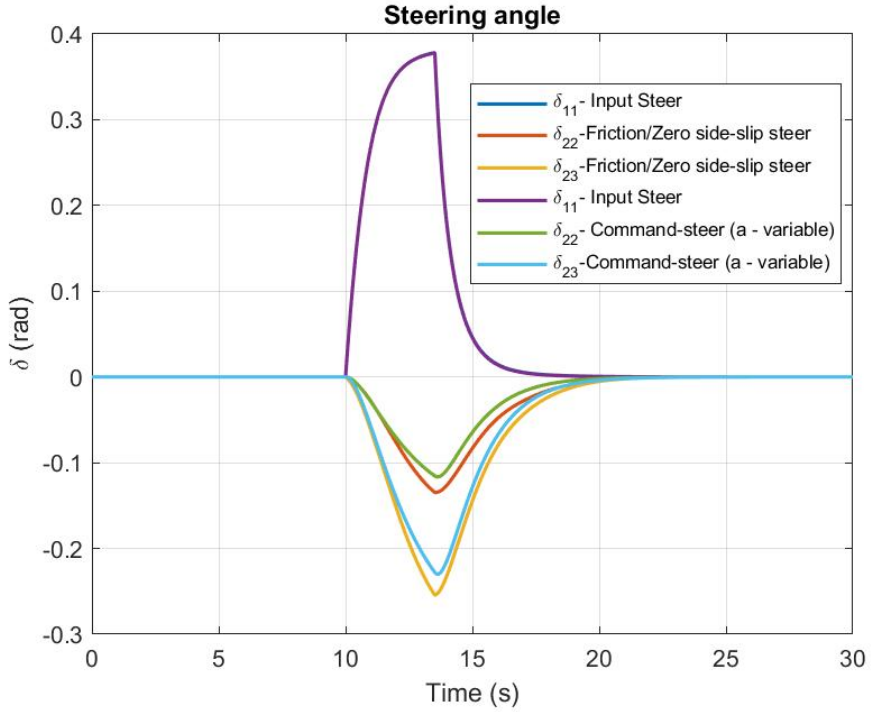

Figure 5.27: A-double :- steering angle for 90 degree & 12.5m radius - first semi-trailer steered

Figure 5.27 is the steering angles on the first axle (δ_{11}) and the two semi-trailer axles (δ_{22} & δ_{23}) of the 1^{st} semi-trailer that are selected to be steered. The steering angles (δ_{22} & δ_{33}) represent the friction steered and algorithm based command steered with variable parameter 'a' models.

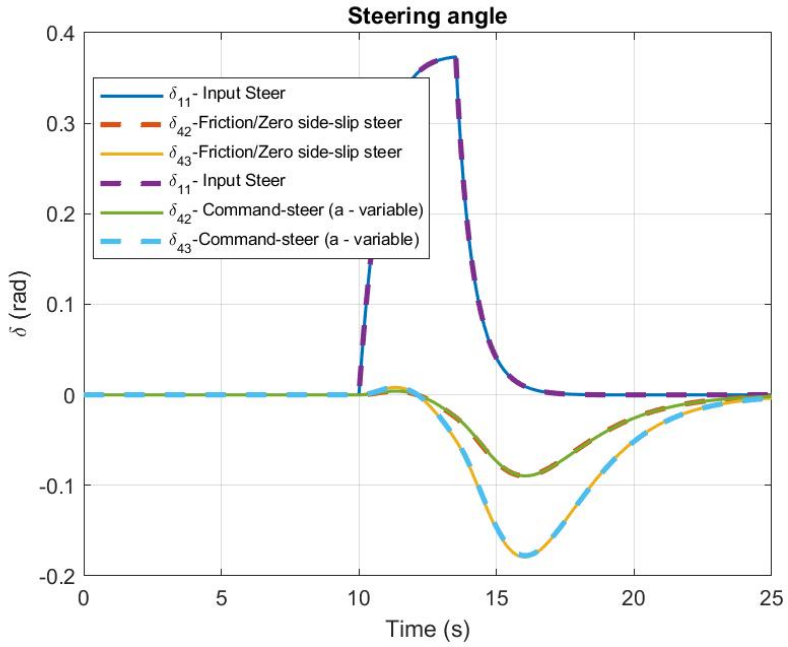

Figure 5.28: A-double :- steering angle for 90 degree & 12.5m radius - second semi-trailer steered

Figure 5.28 is the steering angles on the first axle (δ_{11}) and the two semi-trailer axles (δ_{42} & δ_{43}) of the 2^{nd} semi-trailer that are selected to be steered. The steering angles (δ_{42} & δ_{43}) represent the friction steered and algorithm based command steered with variable parameter 'a' models.

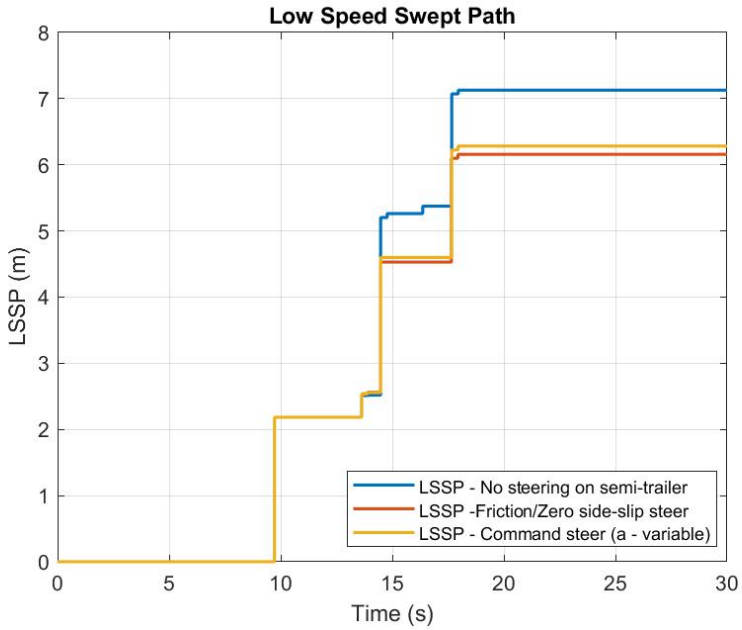

Figure 5.29: A-double :- low speed swept path for 90 degree & 12.5m radius - first semi-trailer steered

The figure 5.29 shows the swept path of the selected vehicle combination from start to end for a defined manoeuvre. It includes the measure of low speed swept path for three different cases for the same vehicle combination. The first case being the non steered axles on semi-trailer and the other two cases with two steered axles ($axle_{22}$ & $axle_{23}$) on 1^{st} semi-trailer for friction-zero side-slip steering and algorithm based command steering with variable parameter 'a' models.

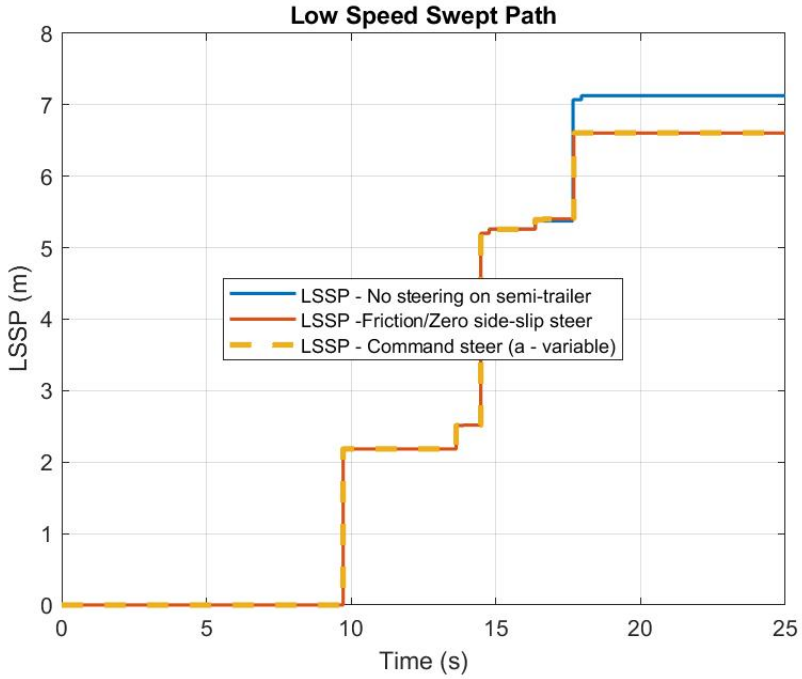

Figure 5.30: A-double :- low speed swept path for 90 degree & 12.5m radius - second semi-trailer steered

The figure 5.30 shows the swept path of the selected vehicle combination from start to end for a defined manoeuvre. It includes the measure of low speed swept path for three different cases for the same vehicle combination. The first case being the non steered axles on semi-trailer and the other two cases with two steered axles ($axle_{42}$ & $axle_{43}$) on 2^{nd} semi-trailer for friction-zero side-slip steering and algorithm based command steering with variable parameter 'a' models.

Figure 5.31: A-double :- distance from coupling to the zero side-slip point (a) on tractor unit for 90 degree & 12.5m radius - first semi-trailer steered

The parameter 'a' which is the distance measure from the fifth wheel coupling and the zero side slip point on the tractor is plotted in the figure 5.31.

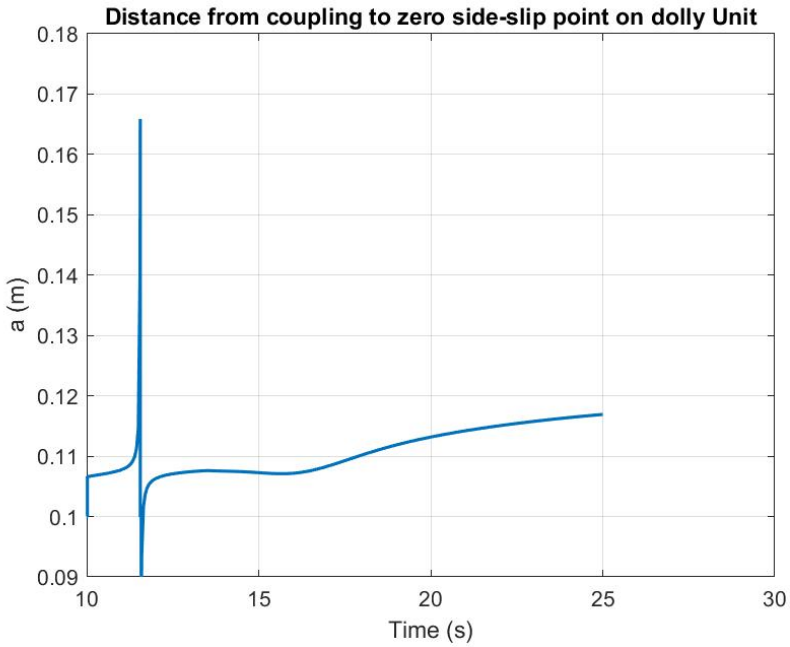

Figure 5.32: A-double :- distance from coupling to the zero side-slip point (a) on dolly unit for 90 degree & 12.5m radius - second semi-trailer steered

The parameter 'a' which is the distance measure from the fifth wheel coupling and the zero side slip point on dolly unit is plotted in the figure 5.32.

The individual swept paths with first and second semi-trailer axles steered individually are tabulated and compared in table 5.13 below. From the table it is clear that the non-steered case has the highest swept path com-pared to the other two semi-trailer steered cases and it can be concluded that if the axles of the trailer are steered it possible to achieve a better swept path compared to non-steered case.

	LSSP (m) - First semi-trailer steered	**LSSP (m) - Second semi-trailer steered**	**LSSP (m) - Both semi-trailer steered**
Non-Steered	7.12	7.12	7.12
friction-zero side-slip Steered	6.15	6.60	5.50
Algorithm Based Command Steered With Variable Parameter a	6.28	6.60	-

Table 5.13: A-double :- low speed swept path for three different concept of low speed steered axles for 90 degree & 12.5m radius - First and second semi-trailer steered

The percentage improvement in swept path for friction-zero side-slip steered and algorithm based command steered compared to non steered case are calculated and tabulated in the table 5.14 for first semi-trailer and second semi-trailer axles steered individually.

	Percentage improvement in LSSP (%) - First semi-trailer steered	**Percentage improvement in LSSP (%) - Second semi-trailer steered**	**Percentage improvement in LSSP (%) - Both semi-trailer steered**
Non-Steered and friction-zero side-slip steered	13.62	7.30	22.75
Non-Steered and Algorithm Based Command Steered With Variable Parameter a	11.8	7.30	-

Table 5.14: A-double :- percentage improvement in low speed swept path for 90 degree & 12.5m radius - First and second semi-trailer steered

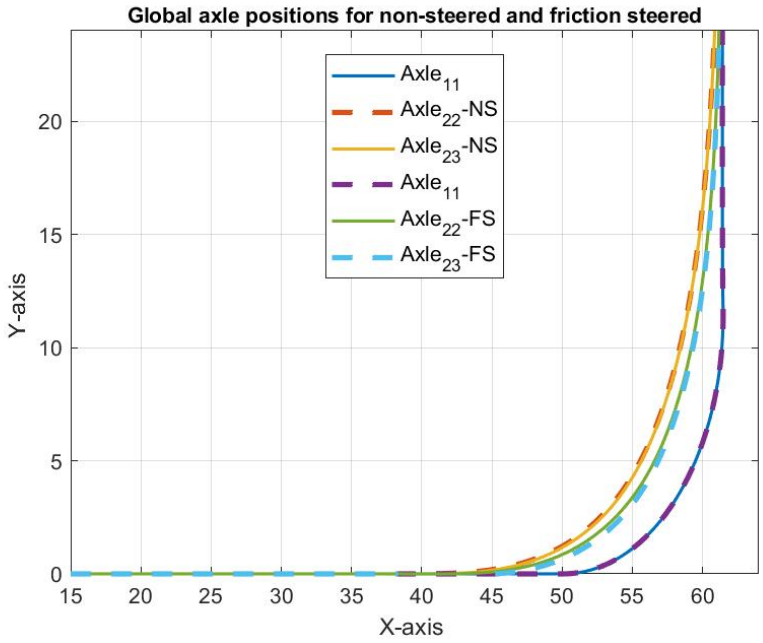

Figure 5.33: A-double - axle global position - friction steered (FS) and non-steered (NS) case for 90 degree turn - first semi-trailer steered

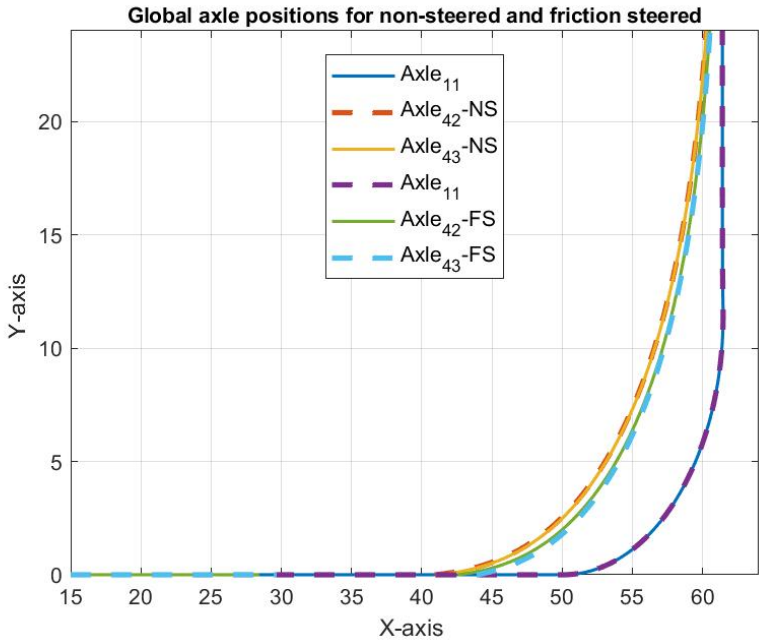

Figure 5.34: A-double - axle global position - friction steered (FS) and non-steered (NS) case for 90 degree & 12.5m radius - second semi-trailer steered

The figure 5.33 & 5.34 represents the axle position/trajectory along the path of the maneuver for first semi-trailer and second semi-trailer steered case respectively for non-steered and friction-zero side-side slip steering model. It is evident that non-

steered axle traces a wider and different trajectory compared to the friction steered axles which in turn reduces the swept path during the corner in both the cases.

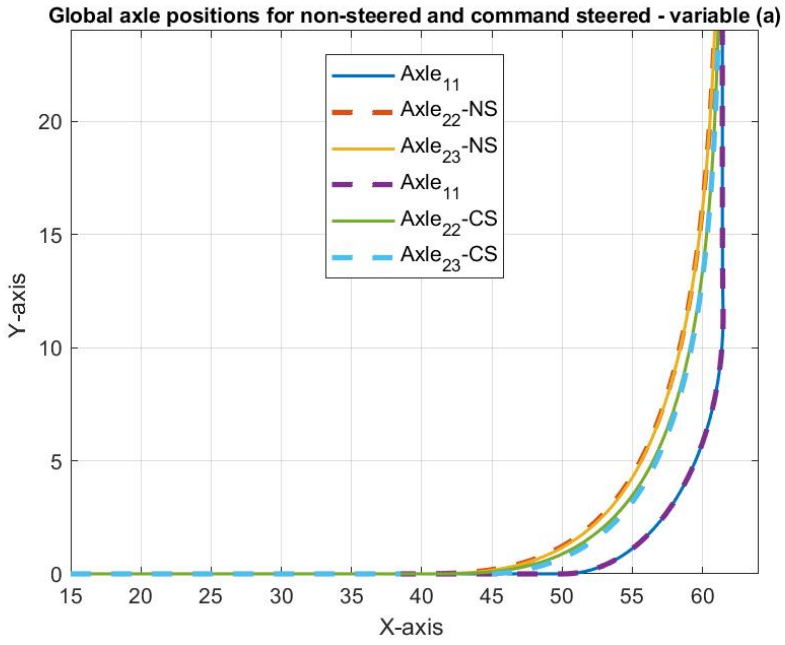

Figure 5.35: A-double - axle global position - command steered (CS) and non-steered (NS) case for 90 degree & 12.5m radius - first semi-trailer steered

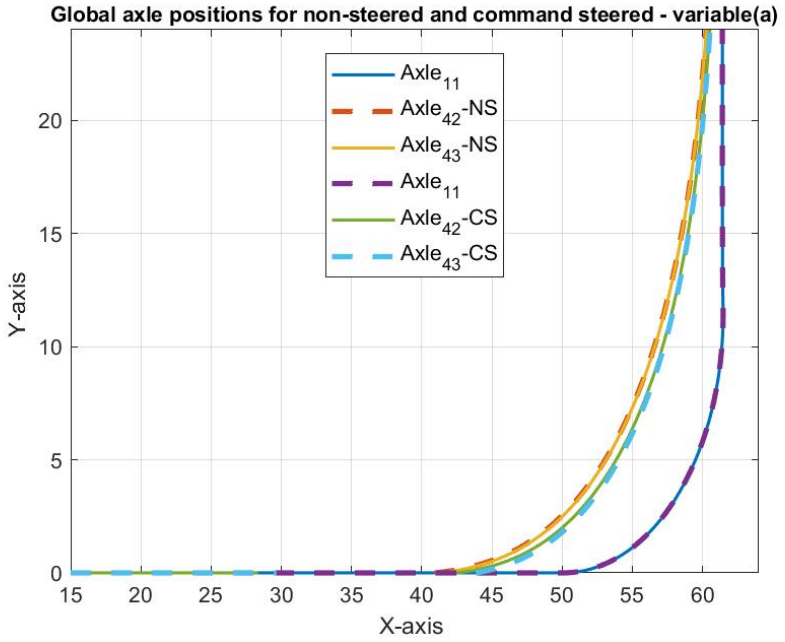

Figure 5.36: A-double - axle global position - command steered (CS) and non-steered (NS) case for 90 degree & 12.5m radius - second semi-trailer steered

The figure 5.35 & 5.36 represents the axle position/trajectory along the path of the

maneuver for first semi-trailer and second semi-trailer steered case respectively for non-steered and command steering model. It is evident that non-steered axle traces a wider and different trajectory compared to the command steered axles which in turn reduces the swept path during the corner in both the cases.

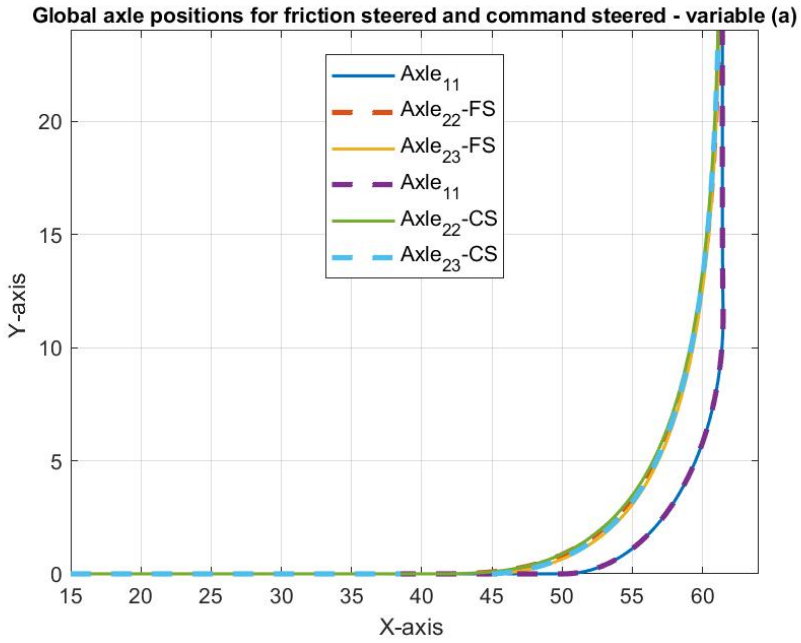

Figure 5.37: A-double - axle global position - command steered (CS) and friction steered (FS) case for 90 degree & 12.5m radius - first semi-trailer steered

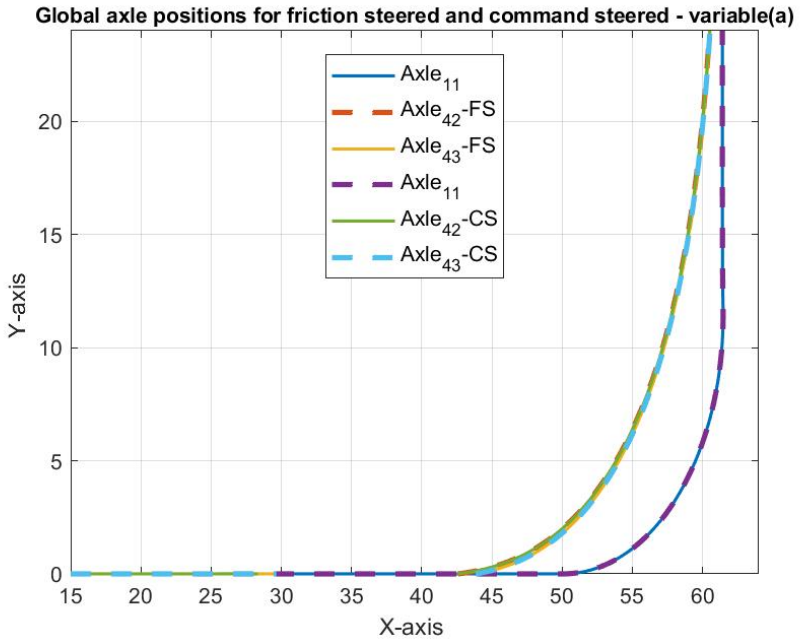

Figure 5.38: A-double - axle global position - command steered (CS) and friction steered (FS) case for 90 degree & 12.5m radius - second semi-trailer steered

The figure 5.37 & 5.38 represents the axle position/trajectory along the path of the maneuver for first semi-trailer and second semi-trailer steered case respectively for friction steering and command steering model. It is evident that command steered and friction steered axles traces almost similar trajectory.

5.1.3.2 Results:- Low speed turn of 180 degree and 12.5 m radius for friction-zero side-slip steer and algorithm based command steer with variable parameter a

.

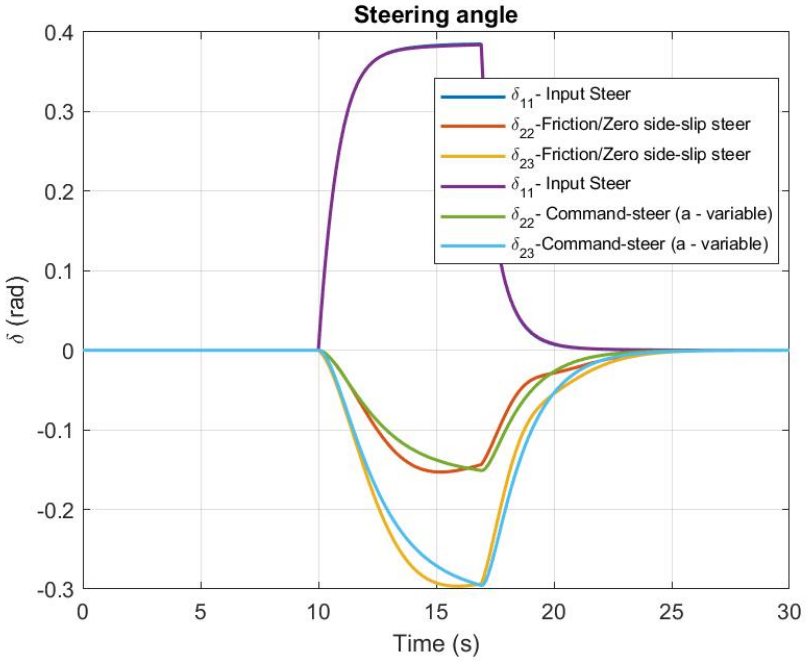

Figure 5.39: A-double :- steering angle for 180 degree & 12.5m radius - first semi-trailer steered

Figure 5.39 is the steering angles on the first axle (δ_{11}) and the two semi-trailer axles (δ_{22} & δ_{23}) of the 1^{st} semi-trailer that are selected to be steered. The steering angles (δ_{22} & δ_{33}) represent the friction steered and algorithm based command steered with variable parameter 'a' models.

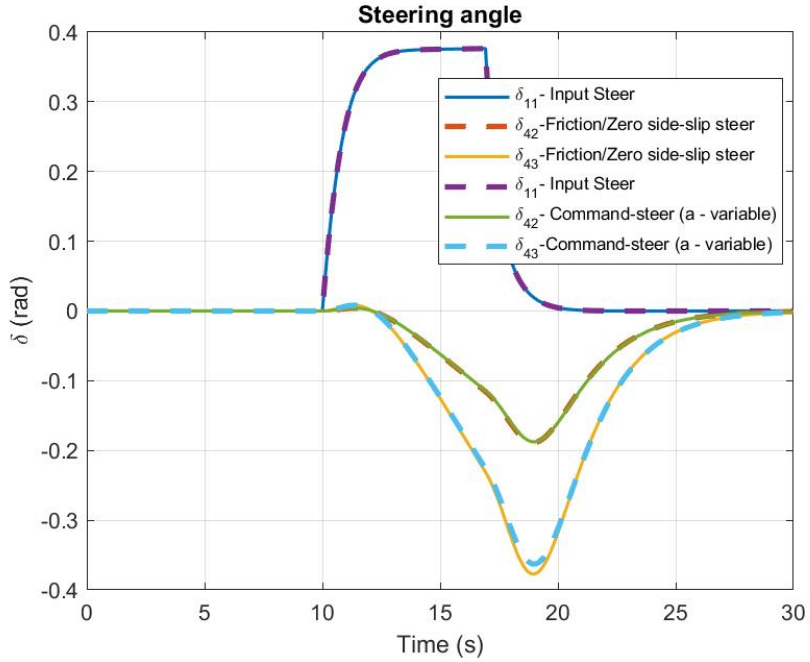

Figure 5.40: A-double :- steering angle for 180 degree & 12.5m radius - second semi-trailer steered

Figure 5.40 is the steering angles on the first axle (δ_{11}) and the two semi-trailer axles (δ_{42} & δ_{43}) of the 2^{nd} semi-trailer that are selected to be steered. The steering angles (δ_{42} & δ_{43}) represent the friction steered and algorithm based command steered with variable parameter 'a' models.

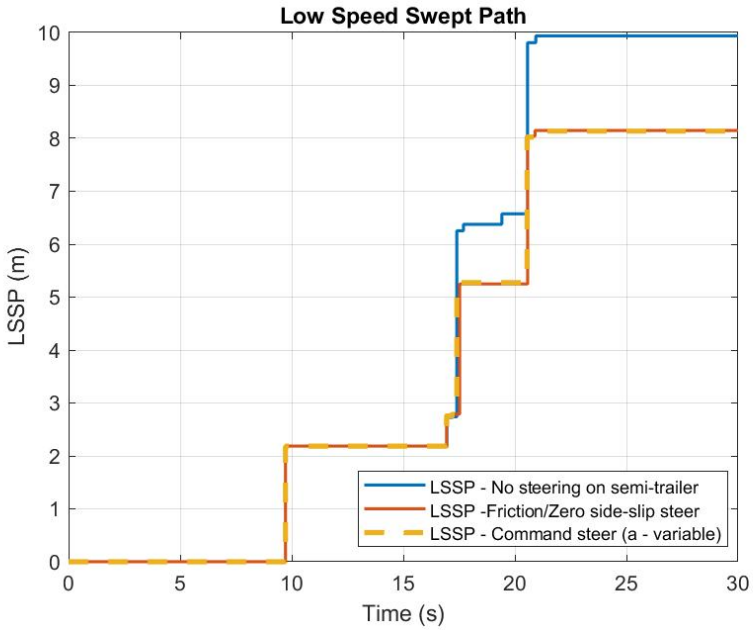

Figure 5.41: A-double :- low speed swept path for 180 degree & 12.5m radius - first semi-trailer steered

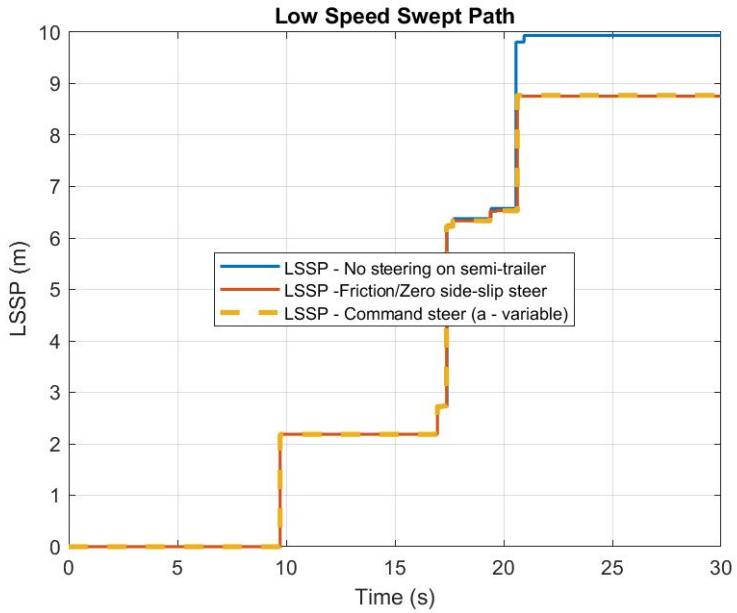

Figure 5.42: A-double :- low speed swept path for 180 degree & 12.5m radius - second semi-trailer steered

The figure 5.41 shows the swept path of the selected vehicle combination from start to end for a defined manoeuvre. It includes the measure of low speed swept path for three different cases for the same vehicle combination. The first case being the non steered axles on semi-trailer and the other two cases with two steered axles ($axle_{22}$ & $axle_{23}$) on 1^{st} semi-trailer for friction-zero side-slip steering and algorithm based command steering with variable parameter 'a' models.

The figure 5.42 shows the swept path of the selected vehicle combination from start to end for a defined manoeuvre. It includes the measure of low speed swept path for three different cases for the same vehicle combination. The first case being the non steered axles on semi-trailer and the other two cases with two steered axles ($axle_{42}$ & $axle_{43}$) on 1^{st} semi-trailer for friction-zero side-slip steering and algorithm based command steering with variable parameter 'a' models.

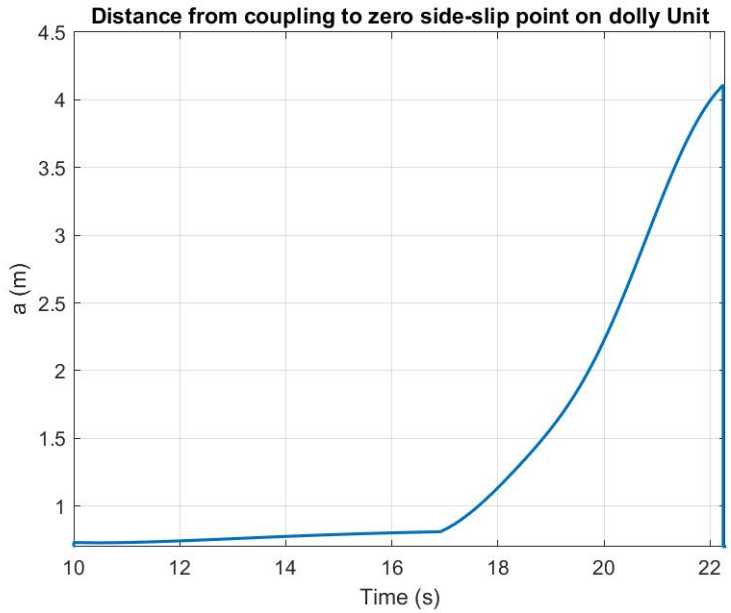

Figure 5.43: A-double :- distance from coupling to the zero side-slip point (a) on tractor unit for 180 degree & 12.5m radius - first semi-trailer steered

The parameter 'a' which is the distance measure from the fifth wheel coupling and the zero side slip point on the tractor is plotted in the figure 5.43.

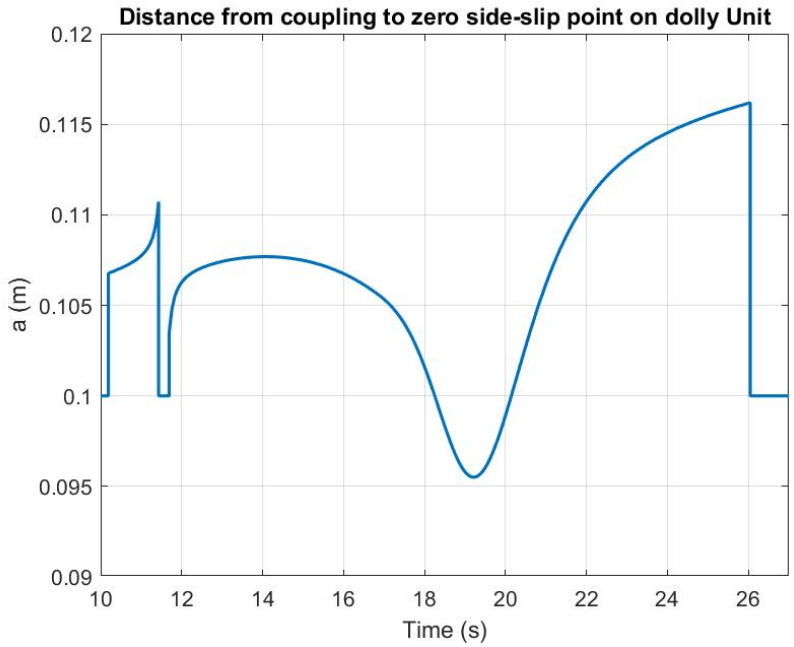

Figure 5.44: A-double :- distance from coupling to the zero side-slip point (a) on dolly unit for 180 degree & 12.5m radiusn - second semi-trailer steered

The parameter 'a' which is the distance measure from the fifth wheel coupling and the zero side slip point on dolly unit is plotted in the figure 5.44.

The individual swept paths with first and second semi-trailer axles steered individually are tabulated and compared in table 5.15 below. From the table it is clear that the non-steered case has the highest swept path com-pared to the other two semi-trailer steered cases and it can be concluded that if the axles of the trailer are steered it possible to achieve a better swept path compared to non-steered case.

	LSSP (m) - First semi-trailer steered	**LSSP (m) - Second semi-trailer steered**	**LSSP (m) - Both semi-trailer steered**
Non-Steered	9.93	9.93	9.93
friction-zero side-slip Steered	8.14	8.75	6.73
Algorithm Based Command Steered With Variable Parameter a	8.13	8.77	-

Table 5.15: A-double :- low speed swept path for three different concept of low speed steered axles for 180 degree & 12.5m radius - First and second semi-trailer steered

The percentage improvement in swept path for friction-zero side-slip steered and algorithm based command steered compared to non steered case are calculated and tabulated in the table 5.16 for first semi-trailer and second semi-trailer axles steered individually.

	Percentage improvement in LSSP (%) - First semi-trailer steered	**Percentage improvement in LSSP (%) - Second semi-trailer steered**	**Percentage improvement in LSSP (%) - Both semi-trailer steered**
Non-Steered and friction-zero side-slip steered	18.02	11.88	32.22
Non-Steered and Algorithm Based Command Steered With Variable Parameter a	18.12	11.68	-

Table 5.16: A-double - axle global position - friction steered (FS) and non-steered (NS) case for 180 degree & 12.5m radius - first semi-trailer steered

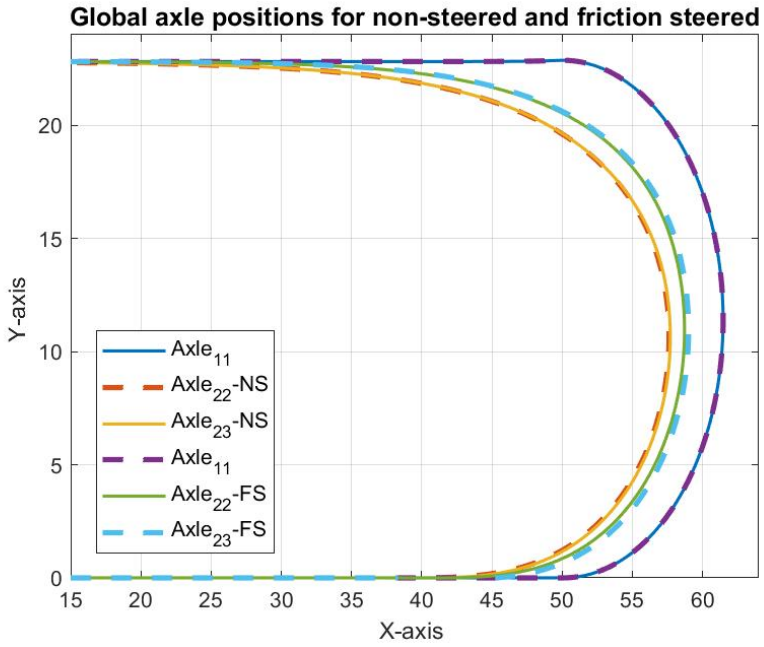

Figure 5.45: A-double - axle global position - friction steered (FS) and non-steered (NS) case for 180 degree & 12.5m radius - first semi-trailer steered

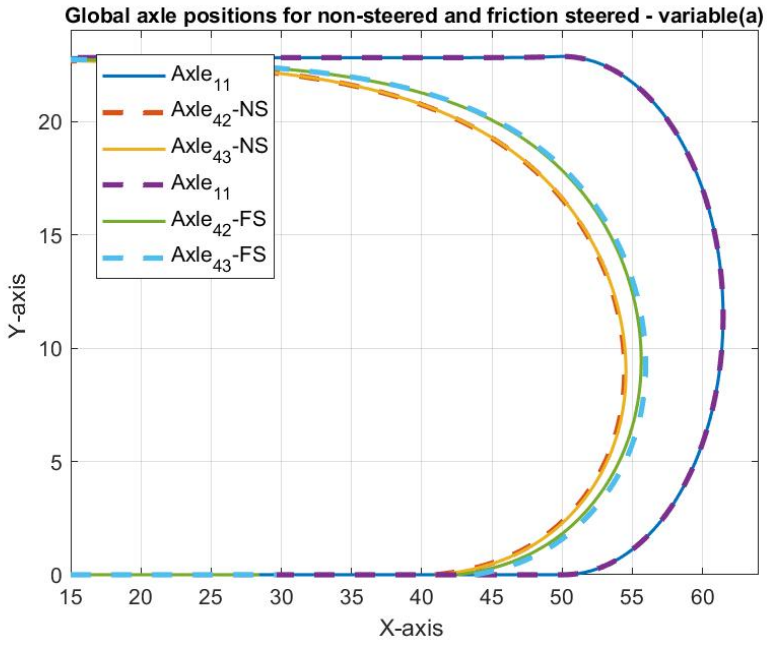

Figure 5.46: A-double - axle global position - friction steered (FS) and non-steered (NS) case for 180 degree & 12.5m radius - second semi-trailer steered

The figure 5.45 & 5.46 represents the axle position/trajectory along the path of the maneuver for first semi-trailer and second semi-trailer steered case respectively for non-steered and friction-zero side-side slip steering model. It is evident that non-

steered axle traces a wider and different trajectory compared to the friction steered which in turn reduces the swept path during the corner in both the cases.

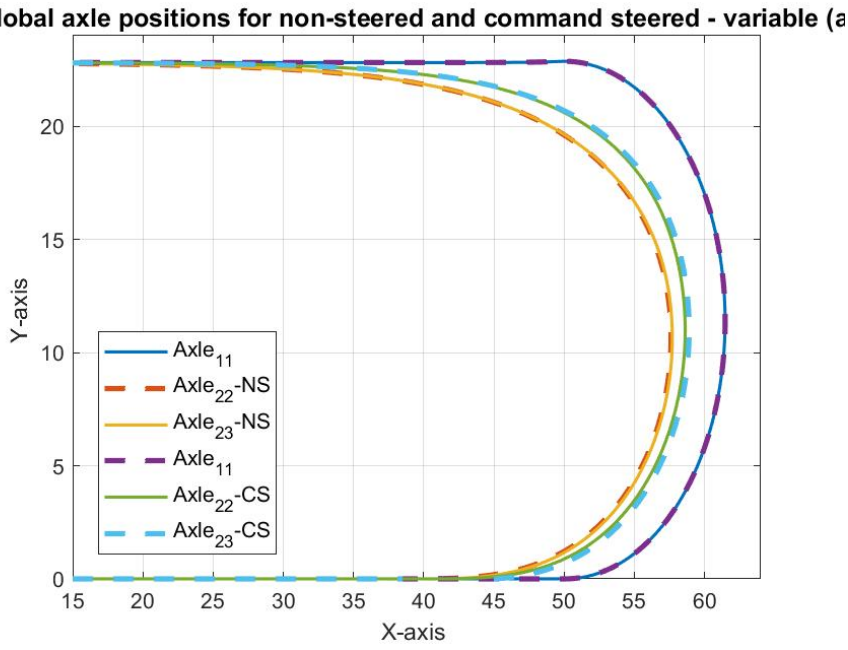

Figure 5.47: A-double :- axle global position - command steered (CS) and non-steered (NS) case for 180 degree & 12.5m radius - first semi-trailer steered

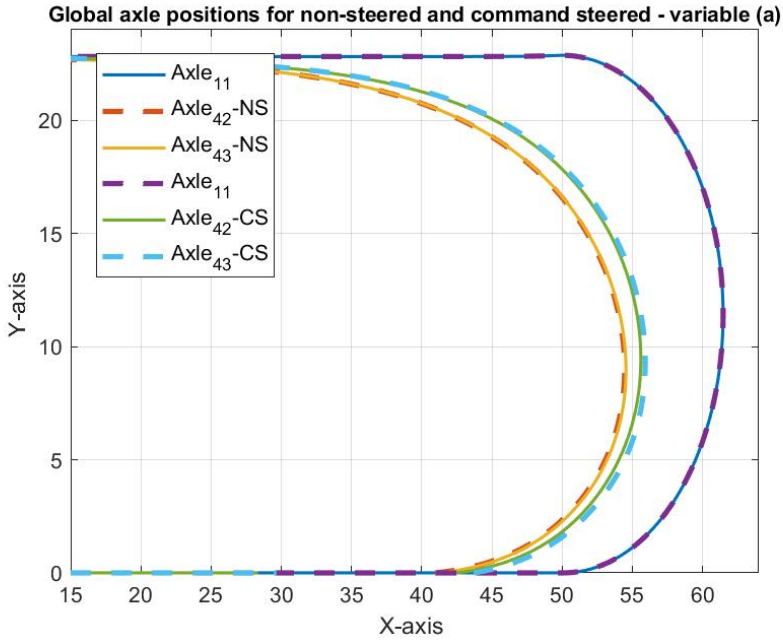

Figure 5.48: A-double - axle global position - command steered (CS) and non-steered (NS) case for 180 degree & 12.5m radius - second semi-trailer steered

The figure 5.47 & 5.48 represents the axle position/trajectory along the path of the

maneuver for first semi-trailer and second semi-trailer steered case respectively for non-steered and command steering model. It is evident that non-steered axle traces a wider and different trajectory compared to the command steered axles which in turn reduces the swept path during the corner in both the cases.

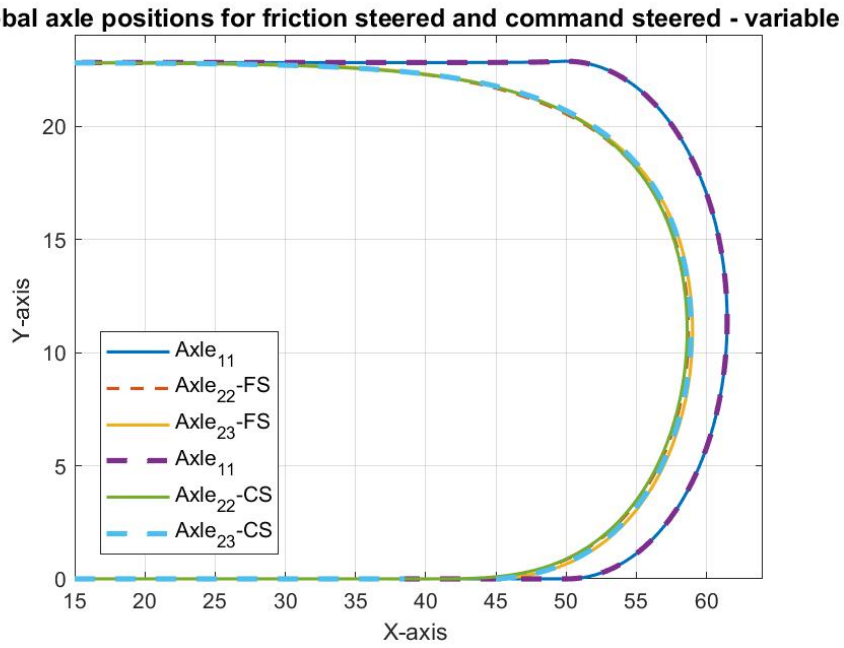

Figure 5.49: A-double :- axle global position - command steered (CS) and friction steered (FS) case for 180 degree & 12.5m radius - first semi-trailer steered

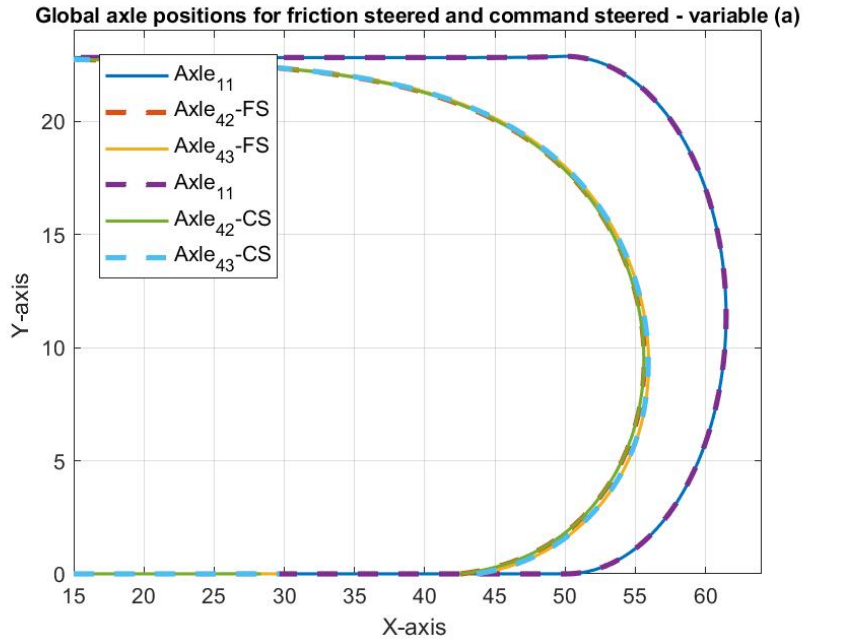

Figure 5.50: A-double :- axle global position - command steered (CS) and friction steered (FS) case for 180 degree & 12.5m radius - second semi-trailer steered

The figure 5.49 & 5.50 represents the axle position/trajectory along the path of the maneuver for first semi-trailer and second semi-trailer steered case respectively for friction steering and command steering model. It is evident that command steered and friction steered axles traces almost similar trajectory.

5.1.4 Results For Steering Models on A-double Vehicle Combination With All Axles Steered Individually

5.1.4.1 Results:- Low speed turn of 90 degree and 12.5 m radius for friction-zero side-slip steer

All the 9 different axles marked in figure 4.4 are low speed steered individually using friction-zero side-slip steering model for A-double vehicle combination and LSSP for each axle case is recorded in table 5.17. From the results it is clear that if only one of the axle needs to be selected to be low speed steered it will be $Axle_{23}$ i,e. the third axle on the first semi-trailer of the A-double combination which has the lowest swept path of 6.67 m during a 90 degree and 12.5 m radius low speed maneuver.

Axle	**LSSP in (m)**	**Percentage change in LSSP compared to non-steered**
$Non - Steered$	7.12	-
$Axle_{13}$	6.98	6.13
$Axle_{21}$	7.45	-4.6
$Axle_{22}$	7.14	-0.28
$Axle_{23}$	6.67	6.3
$Axle_{31}$	7.26	-1.9
$Axle_{32}$	6.98	1.9
$Axle_{41}$	7.36	-3.3
$Axle_{42}$	7.15	-0.42
$Axle_{43}$	6.84	3.9

Table 5.17: Low speed swept path for 90 degree & 12.5m radius - 9 different axles steered individually

5.1.5 Results:- Low speed turn of 180 degree and 12.5 m radius for friction-zero side-slip steer.

All the 9 different axles marked in figure 4.4 are low speed steered individually using friction-zero side-slip steering model for A-double vehicle combination and LSSP for each axle case is recorded in table 5.17. From the results it is clear that if only one of the axle needs to be selected to be low speed steered it will be $Axle_{23}$ i,e. the third axle on the first semi-trailer of the A-double combination which has the lowest swept path of 6.67 m during a 180 degree and 12.5 m radius low speed maneuver.

Axle	**LSSP in (m)**	**Percentage change in LSSP compared to non-steered**
$Non - Steered$	9.93	-
$Axle_{13}$	9.63	3
$Axle_{21}$	10.73	-8
$Axle_{22}$	10.02	- 0.9
$Axle_{23}$	9	9.3
$Axle_{31}$	10.21	-2.8
$Axle_{32}$	9.61	3.22
$Axle_{41}$	10.38	-4.5
$Axle_{42}$	10.00	-0.7
$Axle_{43}$	9.28	6.5

Table 5.18: Low speed swept path for 180 degree & 12.5m radius - 9 different axles steered individually

5.2 Temporarily Lifted Axle Results and Discussion

5.2.1 Results for Lifted Axle Models on Tractor Semi-trailer Vehicle Combination with 1^{st}, 2^{nd} & 3^{rd} Axle Lifted Individually

In this case study tractor semi-trailer vehicle combination which consist of a 3-axle tractor and 3-axle semi-trailer is considered. The effect of lifted axles on the LSSP of the vehicle combination during a low speed curve maneuver is simulated and the results are recorded.

Three different cases are considered to see the effect of LSSP when any of the axle is defined to be lifted and the new vertical forces for all three cases defined in methodology are as follows

- First Semi-trailer Axle Lifted

$$Fz = [72772.825, 89362.567, 89362.567; 0, 87334.026, 87334.026] \tag{5.1}$$

- Second Semi-trailer Axle Lifted

$$Fz = [71632.46, 82560.396, 82560.396; 94706.38, 94706.38, 0] \tag{5.2}$$

- Last Semi-trailer Axle Lifted

$$Fz = [70281.81, 74503.92, 74503.92; 103438.175, 103438.175, 0] \tag{5.3}$$

All three semi-trailer axles are selected to have lifted axles and one of the three are static lifted and the LSSP is recorded in table 5.19.

	LSSP in (m)	**Percentage change compared to Non-lifted (%)**
$Non - Lifted$	5.03	-
$Axle_{21} - Lifted$	5.33	-1.59
$Axle_{22} - Lifted$	4.72	6.16
$Axle_{23} - Lifted$	5.02	0.1

Table 5.19: Low speed swept path for 90 degree & 12.5m radius - Lifted Axle

From the results, if $axle_{22}$ is lifted during the low speed curve maneuver the tractor semi-trailer vehicle combination will have the lowest swept path of 4.72 m and percentage improvement compared to non-lifted case is 6% compared to other two axles i.e. $axle_{21}$ & $axle_{23}$.

6
Conclusion and Limitations

6.1 Conclusions

In this thesis, low speed steered axle were modeled with two different steering methods i,e. friction steered and algorithm based command steer and were implemented in the existing OpenPBS tool to investigate their effect on low speed swept path for different vehicle combinations. Different case studies were investigated for tractor semi-trailer, Nordic and A-double vehicle combinations with different degrees of turn for low speed maneuvers.

For tractor semi-trailer with the last two axles of the semi-trailer steered at low speed, the percentage improvement in the LSSP is 6 % in 90 degree and 8 % in 180 degree turn respectively.

For nordic combination with the last two axles of the semi-trailer steered at low speed, the percentage improvement in the LSSP is 10 % in 90 degree and 15 % for 180 degree turn respectively.

For A-double combination vehicle the percentage improvement in the LSSP with first semi-trailer steered is 13 % and with second semitrailer steered is 7 % in 90 degree turn. The improvement in the LSSP with first semi-trailer steered is 18 % and with second semitrailer steered is 12 % in 180 degree turn.

From the observation of results and discussion of all the case studies defined for three different vehicle combination it can be concluded that the friction-zero side-slip steering method is a conservative representation of algorithm based command steering method with respect to the LSSP. Because the algorithm based command can be tuned with different values of parameter 'a' (distance between the fifth wheel and the zero side slip point on the tractor) to get better LSSP than friction/zero-side slip steering method by sacrificing some tyre wear. Friction/Zero side-slip steering method was selected for implementation in the openPBS tool because it provides similar results as the command steer and also simpler to implement.

The vertical forces are defined as the input parameter in OpenPBS and the driver can input the new vertical loads on the vehicle axles for each transport mission. Temporarily lifted axles are also studied in this thesis work and the new vertical forces are calculated in Matlab and is used as an input to the models.

Tractor-semitrailer combinations with a retractable 1^{st}, 2^{nd} or 3^{rd} axle are considered. The LSSP of the tractor semi-trailer with 1^{st},2^{nd} or 3^{rd} axle lifted is 5.33 m, 4.72 m & 5.02 m respectively and the percentage change of LSSP compared to the non-lifted case is -1.6 % , 6 % & 0.1 % respectively.

6.2 Limitations

- Only two semi-trailer steering methods were investigated in OpenPBS.
- The validation of steering method is only in simulation environment rather than real vehicle tests.
- The command steering is not implemented in OpenPBS because it would require parameters which are not in the vehicle registry, namely the position of the desired zero side-slip point for each unit with low-speed steered axles.
- Other PBS measures i,e. Startability, Gradeability and Rearward Amplification etc are not checked.
- Low speed steered axles on the first unit i,e. last axle on the tractor is not studied with algorithm based command steer in this thesis work.
- When the axle is permanently lifted the new vertical forces calculated are not checked if the the axle group has more load than the one allowed in the regulations.
- The vertical loads of different long combination vehicles remains constant for all different steered axle case studies.

Bibliography

[1] Jacobson, B. et al., 2017. An Open Assessment Tool for Performance Based Standards of Long Combination Vehicles. [Online] Available at: https://research.chalmers.se/en/publication/251269 [Accessed 28 January 2021].

[2] Kharrazi, S., Bruzelius F. & Sandberg U., 2017. Perfromance based standards for high capacity transports in Sweden, FIFFI project 2013-03881 – Final Report" VTI report 948A.

[3] Dymola, Available at: http://www.modelon.com/products/dymola/

[4] Traficom, 2019. Pidemmät ja raskaammat HCT-rekat.https://www.traficom.fi/fi/liikenne/tieliikenne/pidemmat-ja-raskaammat-hct-rekat

[5] ISO 18868:2013, Commercial road vehicles - Coupling equipment between vehicles in multiple combination vehicles - Strength requirements. The International Organization for Standardization.

[6] OECD, 2005. Performance-based Standards for the Road Sector, : Organization for Economic Cooperation and Development (OECD), ISBN 92-821-2337-5.

[7] Mueller, T.H., de Pont J.J. and Baas P.H. (1999). "Heavy vehicle stability versus crash rate".Transport Engineering Research New Zealand Ltd report.

[8] Winkler, C.B., et al. (2000). "Rollover of heavy commercial vehicles". SAE RR-004.

[9] de Pont, J. (2005). "An assessment of heavy truck safety in Tasmania". Transport Engineering Research New Zealand Ltd report.

[10] Kharrazi, S., Karlsson, R., Sandin, J. & Aurell, J., 2015. Performance based standards for high capacity transports in Sweden, Linköping: Swedish National Road and Transport Research Institute (VTI)

[11] Performance Based standards II, Chalmers University of Technology, 2019

[12] Kharrazi, S. et al., 2014. Towards Performance Based Standards In Sweden. VTI.

[13] Jacobson, B. et al., 2017. An Open Assessment Tool for Performance Based Standards of Long Combination Vehicles

[14] Lahti, O., 2018. Suorituskykyperusteiset vaatimukset - Performance based standards.

[15] Lahti, O., 2019. Määräys ajoneuvoyhdistelmien teknisistä vaatimuksista.

[16] Maliheh Sadeghi Kati, Definitions of Performance based characteristics for long heavy vehicle combinations, 2013.

[17] https://www.advantia.com.au/technical/understanding-low-speed-swept-path/

[18] Functional Mock up Interface, Available at: https://www.fmi-standard.org/
[19] WONG, J. Y. Theory Of Ground Vehicles [M]. Canada: John Wiley&Sons. 2001 - ISO 690
[20] Jujnovich, B. and Cebon, D., 2002, June. Comparative performance of semi-trailer steering systems. In Proceedings of the 7th International Symposium on Heavy Vehicle Weights and Dimensions (pp. 195-214). Delft.
[21] ISO 8855:2011 (E), second edition
[22] Jacobson, B. et al., 2017. Performance Based Standards II https://research.chalmers.se/project/8350
[23] Jacobson, B., 2016. Vehicle dynamics compendium for course MMF062; edition 2016. Chalmers University of Technology.
[24] LONG, Michael Thomas. On the statistical correlation between the heave, pitch and roll motion of road transport vehicles. 2016. Doktorarbeit. Victoria University
[25] Odhams, A.M.C., Roebuck, R.L., Jujnovich, B.A. and Cebon, D., 2011. Active steering of a tractor–semi-trailer. Proceedings of the Institution of Mechanical Engineers, Part D: Journal of Automobile Engineering, 225(7), pp.847-869.
[26] Ghandriz, T., Jacobson, B., Laine, L. et al (2020) Impact of automated driving systems on road freight transport and electrified propulsion of heavy vehicles Transportation Research, Part C: Emerging Technologies, 115 http://dx.doi.org/10.1016/j.trc.2020.102610
[27] Kyong-il, K., Hsin, G., Bo, W., Rui, G. and Fan, L., 2016. Active steering control strategy for articulated vehicles [J]. Frontiers of Information Technology & Electronic Engineering, (06), pp.576-586.
[28] Kural, K., Hatzidimitris, P., van de Wouw, N., Besselink, I. and Nijmeijer, H., 2017. Active trailer steering control for high-capacity vehicle combinations. IEEE Transactions on Intelligent Vehicles, 2(4), pp.251-265.
[29] Besselink, I.J.M., Kraaijenhagen, B. and Pauwelussen, J.P., 2014. Greening and safety assurance of future modular road vehicles. In conference; HVTT13; 2014-10-27; 2014-10-30.
[30] LeBlanc, P.A., El-Gindy, M. and Woodrooffe, J.H.F., 1989. Self-steering axles: theory and practice. SAE transactions, pp.156-170.
[31] https://lastbilskalkylator.azurewebsites.net/
[32] Ville sanhahuhta - roll dynamics and tyre relaxation in heavy combination vehicle models for transient lateral manoeuvres. https://hdl.handle.net/20.500.12380/300379
[33] https://www.bpw.de/en/products/axle-running-gears/steering-axles
[34] Ghandriz, T., Jacobson, B., Nilsson, P. et al (2020) Computationally Efficient Nonlinear One-and Two-Track Models for Multitrailer Road Vehicles IEEE Access, 8: 203854-203875 http://dx.doi.org/10.1109/ACCESS.2020.3037035
[35] Ghandriz, T.; Jacobson, B.; Islam, M.; Hellgren, J.; Laine, L. Transportation-Mission-Based Optimization of Heterogeneous Heavy-Vehicle Fleet Including Electrified Propulsion. Energies 2021, 14, 3221
[36] Ghandriz, T. https://research.chalmers.se/publication/520358/file/520358
[37] Surcel, M. and Bonsi, A., "The Impact of Lift Axles on Fuel Economy and GHG Emissions Reduction," SAE Int. J. Commer. Veh. 8(2):673-681, 2015